Chemosphere 148 (2016) 276–291

Contents lists available at ScienceDirect

Chemosphere

journal homepage: www.elsevier.com/locate/chemosphere

Review

Engineered/designer biochar for contaminant removal/immobilization from soil and water: Potential and implication of biochar modification

Anushka Upamali Rajapaksha [a, d], Season S. Chen [b], Daniel C.W. Tsang [b, *], Ming Zhang [c], Meththika Vithanage [d], Sanchita Mandal [e], Bin Gao [f], Nanthi S. Bolan [e], Yong Sik Ok [a, **]

[a] *Korea Biochar Research Center, Kangwon National University, Chuncheon 200-701, South Korea*
[b] *Department of Civil and Environmental Engineering, Hong Kong Polytechnic University, Hung Hom, Kowloon, Hong Kong, China*
[c] *Department of Environmental Engineering, China Jiliang University, Hangzhou, Zhejiang 310018, China*
[d] *Chemical and Environmental Systems Modeling Research Group, National Institute of Fundamental Studies, Kandy, Sri Lanka*
[e] *CERAR, Centre for Environmental Risk Assessment and Remediation, Building-X, University of South Australia, Mawson Lakes, South Australia 5095, Australia*
[f] *Department of Agricultural and Biological Engineering, University of Florida, Gainesville, FL 32611, United States*

HIGHLIGHTS

- Recent developments of engineered biochar for contaminant removal are reviewed.
- Chemical, physical, impregnation, and magnetic approaches improve applicability.
- Immobilization mechanisms of organic/inorganic contaminants are evaluated.
- Outcome-based biochar modifications can enhance environmental remediation.

GRAPHICAL ABSTRACT

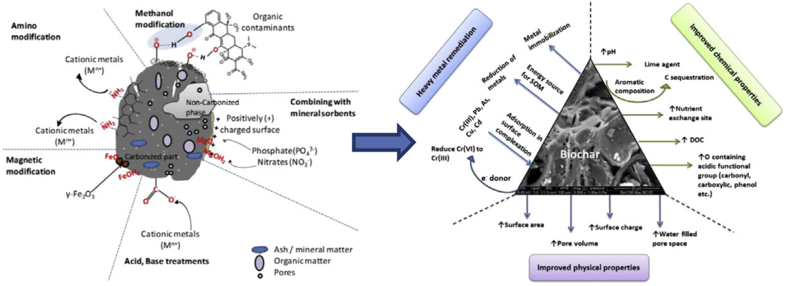

ARTICLE INFO

Article history:
Received 21 September 2015
Received in revised form
8 January 2016
Accepted 11 January 2016
Available online xxx

Handling Editor: X. Cao

Keywords:
Adsorbent
Black carbon
Charcoal
SMART biochar

ABSTRACT

The use of biochar has been suggested as a means of remediating contaminated soil and water. The practical applications of conventional biochar for contaminant immobilization and removal however need further improvements. Hence, recent attention has focused on modification of biochar with novel structures and surface properties in order to improve its remediation efficacy and environmental benefits. Engineered/designer biochars are commonly used terms to indicate application-oriented, outcome-based biochar modification or synthesis. In recent years, biochar modifications involving various methods such as, acid treatment, base treatment, amination, surfactant modification, impregnation of mineral sorbents, steam activation and magnetic modification have been widely studied. This review summarizes and evaluates biochar modification methods, corresponding mechanisms, and their benefits for contaminant management in soil and water. Applicability and performance of modification methods depend on the type of contaminants (i.e., inorganic/organic, anionic/cationic, hydrophilic/hydrophobic, polar/non-polar), environmental conditions, remediation goals, and land use purpose. In general,

---

* Corresponding author. Department of Civil and Environmental Engineering, Hong Kong Polytechnic University, Hung Hom, Kowloon, Hong Kong, China.

** Corresponding author. Department of Biological Environment, Kangwon National University, Chuncheon 200-701, South Korea.

E-mail addresses: dan.tsang@polyu.edu.hk (D.C.W. Tsang), soilok@kangwon.ac.kr (Y.S. Ok).

http://dx.doi.org/10.1016/j.chemosphere.2016.01.043

Sorption
Surface chemistry

modification to produce engineered/designer biochar is likely to enhance the sorption capacity of biochar and its potential applications for environmental remediation.

Contents

1. Introduction

Biochar, a stable carbon (C)-rich by-product synthesized through carbonization of biomass in an oxygen-limited environment (Lehmann and Joseph, 2009) has been recognized as a multifunctional material for energy and environmental applications. Variety of applications include C sequestration (Kuzyakov et al., 2009; Woolf et al., 2010), greenhouse gas emission reduction (Singh et al., 2010), land remediation, contaminant's immobilization (Ahmad et al., 2014; Mohan et al., 2014b) and soil fertilization (Chan et al., 2007, 2008).

The chemical and physical properties of biochar mainly depend on feedstock types and pyrolysis conditions i.e., residence time, temperature, heating rate, and reactor type. Conventional carbonization (i.e. slow pyrolysis), fast pyrolysis, flash carbonization, and gasification are the main thermochemical processes that are widely employed for biochar production (Manyà, 2012). In general, biochar produced at high temperatures (600–700 °C) shows highly aromatic nature with well-organized C layers, but has fewer H and O functional groups due to dehydration and deoxygenation of the biomass (Ahmad et al., 2014; Uchimiya et al., 2011), potentially with lower ion exchange capacities (Novak et al., 2009). On the other hand, biochar produced at lower temperatures (300–400 °C) has more diversified organic characters, including aliphatic and cellulose type structures and contain more C=O and C–H functional groups (Glaser et al., 2002; Novak et al., 2009). The complex and heterogeneous chemical and physical composition of biochar provides an excellent platform for contaminants removal through sorption (Park et al., 2015a; Vithanage et al., 2015a). In spite of considerable scientific work on the uses of biochar for environmental uses, extensive attention has recently been focused on the modification of biochar with novel structures and surface properties in order to enhance its remediation efficacy and environmental benefits (Ok et al., 2015). It is timely and essential to review the scientific literature on novel modifications and their effects. For the sake of facilitating future design and improving performance and widespread use of -engineered char materials like biochar for environmental applications and remediation, this review paper provides a timely comprehensive summary and critical evaluation of the principles and applications of various surface modifications on biochar in view of up-to-date available peer-reviewed research work.

2. Modification methods for engineered/designer biochar preparation

Available modification methods that have been investigated in previous literature are summarized in Table 1, which can be divided into four main categories, i.e., chemical modifications, physical modifications, impregnation with mineral sorbents, and magnetic modifications (Fig. 1).

2.1. Chemical modification

Chemical modification process involves both one step modification and two-step modification process. The carbonization and activation steps are achieved simultaneously during one-step chemical activation in the presence of an activating chemical agent. Two-step chemical activation involves carbonization of raw feedstock followed by activation of the carbonized product by mixing with a chemical agent or pretreatment of precursors before the carbonization process (Azargohar and Dalai, 2008; Qian et al., 2015).

2.1.1. Acid/base treatment and chemical oxidation process of biochar

Treatments to the carbon precursors or resulted biochar after pyrolysis during chemical modification have been reported to effect profoundly on biochar performance as an amendment or sorbent (Kasparbauer, 2009). All treatments create additional costs but are beneficial in the end due to enhanced properties. Treatment by chemical modification is generally carried out by addition of acids

Table 1

Different modification methodologies of biochars, production conditions, contaminant removals (mechanisms) and their applications with representative publication details.

Modification method	Biochar feedstock	Production temperature	Target sorbate	Enhancement	Mechanism	References
Chemical modifications						
Chemical oxidation ($KMnO_4$, HNO_3, or NaOH)	Bamboo	550 °C	Furfural	Chemical treatments inhibited sorption of furfural	Introduction of a large number of acidic functional groups on biochar surface; HNO_3 was more effective than $KMnO_4$. By contrast, NaOH and heat treatments increased basicity of biochar	Li et al. (2014d)
H_2O_2 modification	Peanut hull	300 °C	Pb^{2+},Cu^{2+}, $Ni^{2+}$and Cd^{2+}	Enhanced Pb^{2+} sorption from 0.88 to 22.82 mg g^{-1}, comparable to commercial activated carbon	Increased O-containing functional groups, particularly carboxyl groups, on hydrochar surfaces	Xue et al. (2012)
Chemically modified (10% H_2SO_4 or 3 M KOH)	Rice husk	450–500 °C	Tetracycline	Exhibited better sorption performance (58.8 mg g^{-1}) than the other two biochars	Possessed larger surface area than those of raw and acid treated biochars	Liu et al. (2012)
NaOH activation	Pine chip	300 °C	Diclofenac (DCF), naproxen (NPX), and ibuprofen (IBP)			Jung et al. (2015)
KOH modification	Municipal solid waste	400, 500 and 600 °C	As^{5+}	More than 1.3 times adsorption than unmodified biochars	Increase of surface area and changes of porous texture, especially functional groups on the surface of activated biochars	Jin et al. (2014)
Acid activated biochar		300 and 700 °C	Sulfamethazine (SMT)	Extensive increase in the BET surface area and enhancement in sorption of sulfamethazine		Vithanage et al. (2015b)
Activated with HCl, and coated with iron ($FeCl_3$ $.6H_2O$)	Wheat straw	450 °C	Nitrate and phosphate	Significant increase of sorption after coating with iron		Li et al. (2014c)
Phosphoric acid-microwave method	Pine tree sawdust	550 °C	Fluoride		Increasing F^- sorption resulting from chemistry reaction and increased specific surface area	Guan et al. (2014)
Chemically modified biochar ($Mg(OH)_2$)	Conocarpus wastes	400 °C	Fe^{2+}	Higher sorption capacities for chemically modified biochar (84.6–99.8%) followed by unmodified biochar (38.3–97.6%)	Mineral components such as calcite, silicate and $Mg(OH)_2$ in biochars samples accelerate the oxidation of Fe^{2+} and form precipitate of Fe^{3+} hydroxides	Usman et al. (2013)
Methanol-modified biochar	Rice husk	450–500 °C	Tetracycline (TC)	Approximately 45.6% enhancement of sorption capacity in 12 h and 17.2% at equilibrium	Due to change in O- containing groups	Jing et al. (2014)
Amino-modified biochar	Saw dust	500 °C	Cu^{2+}	Enhanced sorption up to 5-folds and 8-folds for batch and fixed-bed experiments	Amino moiety efficiently complexes with heavy metals in view of high stability constants of metal complexes	Yang and Jiang (2014)
Polyethylenimine modified biochar	Rice husk	450–500 °C	Cr^{6+}	Maximum sorption capacity of 435.7 mg g^{-1}, compared to that of unmodified biochar (23.09 mg g^{-1})	Introduction of amino group facilitate chemical reduction of Cr^{6+} and increase sorption capacity	Ma et al. (2014)
Carbon nanotube-modified biochars (surfactant-aided dispersion)	Hickory or bagasse	600 °C	Pb^{2+} and sulfapyridine			Inyang et al. (2015)
Hybrid multi-walled carbon nanotube (CNT)-coated biochars	Hickory chips and sugarcane bagasse	600 °C	Methylene blue	Highest sorption capacity among all the sorbents	Biochar-CNT-1% have better thermal stability, higher surface area, and larger pore volume	Inyang et al. (2014)
Biochar coated silica material	Rice husk		Characterization of the material			Li et al. (2012)
Fe(III) coated biochar	Empty fruit bunch and rice husk		As^{3+} and As^{5+}	Improvement of sorption capacities	Interactions with FeOH and $FeOH_2^+$ groups	Samsuri et al. (2013)
Physical modification						
Steam activation	Maize stover and *Eucalyptus* wood	350 and 550 °C	Emission of N_2O and CH_4		Suppress CH_4 and N_2O emission	Fungo et al. (2014)
Steam and KOH activation	whitewood (Spruce)					Azargohar and Dalai (2008)
Steam activation	Invasive plant (Burcucumber)	300 and 700 °C	Sulfamethazine (SMT)	55% increase in sorption capacity		Rajapaksha et al. (2015)
Steam activation	chicken litter, alfalfa stems, switchgrass, corn cob and stover, guayule	500 °C	Cu^{2+}			Lima et al. (2010)

Table 1 (*continued*)

Modification method	Biochar feedstock	Production temperature	Target sorbate	Enhancement	Mechanism	References
	bagasse and shrub, and soybean straw					
Steam activation	Tea waste	300 and 700 °C	Sulfamethazine (SMT)	Highest SMT sorption among all biochars	Due to its largest surface area and pore volume	Rajapaksha et al. (2014b)
Modification by high temperature CO_2–ammonia mixture	Cotton stalk	500–900 °C	CO_2		Ammonia reacts with biochars and introduce nitrogen functional groups for CO_2 sorption at 120 °C	Zhang et al. (2014b)
NH_3/CO_2 Modification	Cotton stalk	500–900 °C	CO_2		NH_3 reacts with biochar surface, introducing the nitrogen functional groups; CO_2 modification forms more micropore	Xiong et al. (2013)
Impregnation with mineral sorbents						
MnOx-loaded biochar	Corn straws	600 °C	Cu^{2+}	Much higher sorption capacity; maximum sorption capacity as high as 160 mg g^{-1}	Formation of innersphere complexes with MnO_x and O- containing groups	Song et al. (2014)
Clay-biochar composites	Bamboo, bagasse, and hickory chips	600 °C	Methylene blue	Increase of sorption capacities by about 5 times	Ion exchange (with clay) and electrostatic attraction (with biochar)	Yao et al. (2014)
Porous MgO-biochar nanocomposites			Phosphorus and nitrates			Zhang et al. (2012a)
Mg-biochar nanocomposite	Mg enriched tomato leaves	600 °C	Phosphorus	Maximum sorption capacity >100 mg g^{-1}	Precipitation of P through chemical reaction with Mg particles and surface deposition of P on Mg crystals on biochar surfaces	Yao et al. (2013a)
Mg-biochar nanocomposite	Mg-accumulated tomato tissues	600 °C	Phosphate (PO_4^{3-})	88.5% removal of P from solution	Nanoscale $Mg(OH)_2$ and MgO particles as main sorption sites for aqueous phosphate	Yao et al. (2013b)
Chitosan-modified biochars	Bamboo, sugarcane bagasse, hickory wood, and peanut hull	600 °C	Pb^{2+}, Cu^{2+}, and Cd^{2+}	Enhanced removal of three metals		Zhou et al. (2013)
Mg–biochar nanocomposites	Sugar beet tailings		Phosphorus	High sorption capacity >100 mg g^{-1}	Presence of the nanosized MgO particles on the biochar surfaces as active sorption sites for aqueous phosphorus	Yao et al. (2011b)
Magnesium modified biochar	Corn	300, 450, and 600 °C	Phosphorus			Fang et al. (2014)
Mineral addition (kaolin, calcite ($CaCO_3$), and calcium dihydrogen phosphate [$Ca(H_2PO_4)_2$])	Rice straw	200, 300, 400 and 500 °C	C retention	Three minerals, especially $Ca(H_2PO_4)_2$, were effective for increasing carbon retention and strengthening biochar stabilization	Enhanced carbon retention and stability of biochar with mineral treatment due to enhanced formation of aromatic C	Li et al. (2014a)
Aluminum-modified crop straw-derived biochars	Rice straw, peanut straw, soybean straw	750 °C	As^{5+}	Al(III)-modified biochars sorbed 445–667 mmol kg^{-1} at pH 5.0, in contrast to negligible sorption on unmodified biochars	Inner-sphere complexes with Al hydroxides on the surfaces of biochars	Qian et al. (2013)
Manganese oxide-modification	Pine wood	600 °C	Arsenic (As^{5+}) and lead (Pb^{2+})	Sorption capacities of As^{5+} increased by about 3.0 and 4.7 times, while those of Pb^{2+} increased by about 2.1 and 20.0 times	Presence of birnessite particles showed strong interactions with heavy metals	Wang et al. (2015a)
Granulation of biochar powder followed by ferric loading	Cotton stalk	350 °C	Phosphate	Increased phosphate sorption capacity from 0 to 0.963 mg g^{-1}	Integration of porous property of biochar, high sorption capability of ferric oxides, and excellent flow characteristics of granular particles	Ren et al. (2015)
Ca and Fe modified biochars	Rice husk	300 °C	Arsenic (As^{5+}) and chromium (Cr^{6+})	More than 95% removal	Heavy metal precipitation as well as electrostatic interactions	Agrafioti et al. (2014)
Biochar supported nanoscale zerovalent iron (nZVI) composite	Rice hull	350 °C	Trichloroethylene (TCE)	Degradation efficiency of TCE (0.15 mmol L^{-1}) was 99.4% in the presence of nZVI/biochar (4.5 mmol L^{-1}, nZVI to biochar mass ratio was 1:5) and persulfate (4.5 mmol L^{-1}) within 5 min	Large specific surface area and O-containing functional groups of nZVI/biochar enhanced SO_4 generation and accelerated TCE degradation	Yan et al. (2015a)
Fe impregnated biochar	Hickory chips	600 °C	Arsenic	Maximum sorption capacity of 2.16 mg g^{-1} compared to negligible sorption onpristine biochar	Chemisorption mechanism on Fe impregnated biochar	Hu et al. (2015)
Magnetic modification						
Magnetic biochars (chemical co-	Orange peel	250, 400 and 700 °C	Naphthalene (NAPH) and p-nitrotoluene (p-			Chen et al. (2011)

(*continued on next page*)

Table 1 (*continued*)

Modification method	Biochar feedstock	Production temperature	Target sorbate	Enhancement	Mechanism	References
precipitation of Fe^{3+}/Fe^{2+}			NT) and phosphates			
Magnetic biochar/γ-Fe_2O_3 composite	Cotton wood	600 °C	Arsenic	Maximum sorption capacity of 3147 mg kg^{-1}	Nano-colloidal structures of well dispersed γ-Fe_2O_3 particles on both surface and interior of biochar matrix	Zhang et al. (2013a)
Magnetic biochars	Oak wood and oak bar	400–450 °C	Cd^{2+} and Pb^{2+}			Mohan et al. (2014a)
Magnetic biochar/ZnS composites	Rice hull	400 °C	Pb^{2+}	Significantly improved sorption capacity		Yan et al. (2015b)
Magnetic biochar	Pinewood	600 °C	Arsenic (As^{5+})	Greater removal of As^{5+} from aqueous solution	γ-Fe_2O_3 particles on biochar surface served as sorption sites through electrostatic interactions	Wang et al. (2015b)

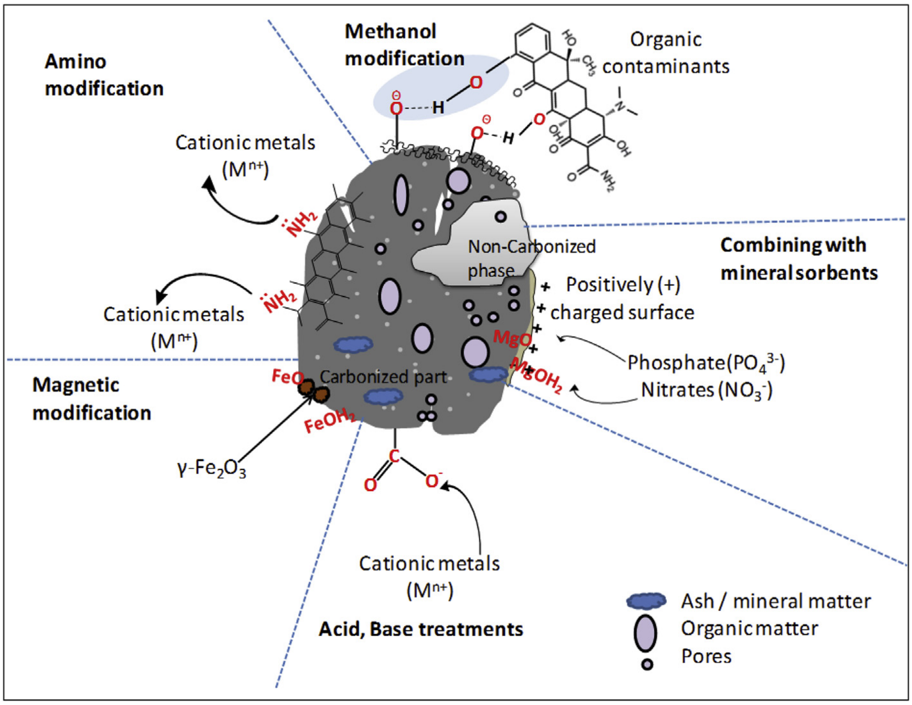

Fig. 1. Schematic diagram of biochar modifications.

or bases. In addition, intentional oxidation using hydrogen peroxide (H_2O_2), potassium permanganate ($KMnO_4$), ammonium persulfate [$(NH_4)_2S_2O_8$] and ozone (O_3) have been used to modify surface functional groups (Cho et al., 2010; Uchimiya et al., 2011).

Washing with strong acids (such as phosphoric – H_3PO_4, sulfuric – H_2SO_4, nitric – HNO_3, and hydrochloric – HCl acid) has been studied for the purpose of aqueous oxidation, which can enhance surface acidities and modify porous structure of biochar (Lin et al., 2012). Table 2 summarizes the acid/base treatment and chemical oxidation methodologies of biochar reported in literature. Phosphoric acid is one of the most commonly used activating agents for chemical modification and is more environmental-friendly than other corrosive and hazardous reagents such as $ZnCl_2$ (Guo and Rockstraw, 2007; Sun et al., 2011). Phosphoric acid can decompose lignocellulosic, aliphatic, and aromatic materials while forming phosphate and polyphosphate cross bridges to avoid shrinkage or contraction during the porosity development (Fierro et al., 2010; Klijanienko et al., 2008; Yang et al., 2011).

Other mineral acids such as HNO_3, H_2SO_4 and HCl have also been widely used for modification of biochar. The oxidation with HNO_3 treatment has been shown to cause degradation of the micropore wall due to its erosive nature, resulting in a decrease of total surface area (Stavropoulos et al., 2008). Similarly, H_2SO_4 treatment resulted in a decrease in the porosity of biochar from 10 to 40% and improved the size distribution of heterogeneous micropore (Yakout et al., 2015). Dehydration of H_2SO_4 during pyrolysis could be detrimental to the development of surface area due to excess water vapor movement towards the surface structure (Guo et al., 2005). Organic acids such as oxalic enhance sorption of pollutants through ligand- and proton-promoted processes (Vithanage et al., 2015b). Although pretreatment with 10% H_2SO_4 at 60 °C was observed to impose little effect on C and O_2 contents (Fan et al., 2010), a combined treatment of 30% H_2SO_4 and oxalic acid demonstrated a 250-fold increase of surface area compared to the unmodified biochar (Vithanage et al., 2015b). Li et al. (2014c) also reported that the modification of wheat straw-derived biochar with 1 M and 6 M HCl introduced more heterogeneous pores than the unmodified ones. Indigenous inorganic/metal impurities can also be effectively

Table 2
Acid/base treatment and chemical oxidation process of biochar.

Modification	Feedstock	Liquid-solid ratio	Concentration	Temperature	Time	pH	References
H_3PO_4 KOH	*Acacia saligna* biochar; sawdust biochar; Jarrah biochar	40 mL g^{-1}	1 M 0.1 M	90 °C	1 h	N/A	Lin et al. (2012)
H_2SO_4 + oxalic acids	Burcucumber plant	100 mL: 5 g	30%	Room temperature	4 h	N/A	Vithanage et al. (2015b)
H_2SO_4 KOH	Rice husk derived biochar	200 mL: 20 g	10% (v/v) 3 M	60–70 °C	1 h	5–9	Liu et al. (2012)
KOH	Alamo switchgrass hydrothermal biochar	500 mL: 2 g	2 M	Room temperature	1 h	5, 7	Regmi et al. (2012)
NaOH	Bamboo charcoal	N/A	10%	60 °C	6 h	N/A	Fan et al. (2010)
H_2O_2 (Oxidation)	Bamboo charcoal	1 mL g^{-1}	15–30%	Room temperature	12 h	N/A	Tan et al. (2011)
H_2O_2 (Oxidation)	Peanut hull hydrochar	20 mL: 3 g	10%	Room temperature	2 h	N/A	Xue et al. (2012)
(1) H_2SO_4 + HNO_3 (2)							

NH_4OH + $Na_2S_2O_4$ + acetic acid (Amination)Saw dust biochar(1) 50 mL +50 mL: 6 g;
(2) 20 mL, 28 g, 120 mL: 5 g(1) conc. acids;
(2) 15 M, 2.9 M(1) Room temperature
(2) Reflux with glacial acetic acid at 100 °C(1) 2 h,
(2) 15 min, 20 h, 5 h5Yang and Jiang (2014)

removed by acid washing (Liou and Wu, 2009). In general, it is recognized that treatment with strong acids can introduce the acidic functional groups such as amine, carboxylic groups onto the carbonized surface, thereby enriching the metal sorption affinity and capacity through cation exchange and surface complexation with these additional active sites.

Alkali activation of biochar using potassium hydroxide (KOH) and sodium hydroxide (NaOH) can increase the O content and surface basicity (Fan et al., 2010; Li et al., 2014c), while dissolving ash and condensed organic matter (e.g., lignin and celluloses) to facilitate subsequent activation (Lin et al., 2012; Liou and Wu, 2009; Liu et al., 2012). A two-stage KOH activation process of pre-carbonized precursors could produce a larger surface area with additional surface hydroxyl groups (Basta et al., 2009; Oh and Park, 2002). Compared to KOH, NaOH is deemed more economical and less corrosive for carbon activation (Cazetta et al., 2011). However, it should be noted that NaOH modification at a lower temperature (60–100 °C) was found to result in a smaller surface area (less than 1 m^2 g^{-1}) with only few micropores (Fan et al., 2010; Li et al., 2014c). There was a marginal change in the fraction of functional groups on the biochar surface because the content of graphite C was predominant (Fan et al., 2010; Regmi et al., 2012). Consequently, there should be a careful balance between the physical properties (e.g., stability) and surface chemistry of biochar in the selection of pretreatment methods.

Biochar with extremely high surface areas have been reported after treating with KOH or NaOH (Chia et al., 2015). Potassium species (K_2O, K_2CO_3) may be formed during activation as a result of intercalation of K^+ in the layer of the crystallites that form the condensed C structure. These species may diffuse into the internal structure of biochar matrix widening existing pores and creates new pores of the product (Mao et al., 2014).

Chemical modification of biochar may enhance its contaminant sorption ability by creating additional and abundant sorption sites on increased surface areas, rendering biochar surface more conducive to electrostatic attraction, surface complexation, and/or surface precipitation, as well as enabling greater sorption affinity through stronger interactions with specific surface functional groups. Table 3 and Fig. 2 summarize the enhanced performance and mechanisms of chemically modified biochar for solute adsorption. Acid pretreatment and chemical oxidation of biochar generally enhanced metal removal. For instance, H_2O_2 oxidation increased the amount of carboxyl groups on biochar surface and provided additional cation exchange site for surface complexation of Pb^{2+} and Hg (Tan et al., 2011; Xue et al., 2012), which were comparable or even superior to commercial activated carbons. The H_2O_2 modified biochar showed enhanced Pb^{2+} sorption with a sorption capacity of 22.8 mg g^{-1}, which was more than 20 times of that of the unmodified biochar (0.88 mg g^{-1}) due to increased O-containing functional group.

Although the surface functionalities remained mostly unchanged after the modification by KOH activation, Cu^{2+} and Cd^{2+} sorption was significantly enhanced which may be due to large surface area and high amounts of O-containing functional groups (Regmi et al., 2012). In addition to carboxyl groups, amination modification of biochar also significantly enhanced the Cu^{2+} sorption via strong surface complexation with amino functional groups (Yang and Jiang, 2014), which was highly selective and minimally affected by competing cations. The modified biochar by KOH significantly enhanced its sorption capacity to As^{5+} due to increase of surface area and pore volume and alternation of functional groups on the surface (Jin et al., 2014).

Removal of organic pollutants could be enhanced by the π–π electron donor acceptor interaction between biochar and aromatic rings of organic compounds (Fan et al., 2010; Liu et al., 2012; Rajapaksha et al., 2014b). Table 3 shows that the reported capacity for tetracycline removal by KOH-modified biochar (58.52 mg g^{-1}) was significantly larger than most studies (4.3–54 mg g^{-1}) (Liu et al., 2012), while the observed value for chloramphenicol removal by NaOH-modified biochar was significantly higher than the unmodified biochar (Fan et al., 2010). On the other hand, urea modification could introduce N functional groups (pyridinic groups) and increase the surface basicity, thus enhancing π–π dispersion forces for phenol uptake (Stavropoulos et al., 2008). Besides, acid modification could also enrich the content of carbonyl groups for π–π interaction. Vithanage et al. (2014; 2015b)showed that biochar modified with sulfuric and oxalic acids provided a promising result of 183–229 L kg^{-1} sulfamethazine sorption in different types of soils, probably because of development of surface functional groups and increase in surface areas of modified biochar (Table S1).

2.1.2. Modification of functional groups (carboxylation and amination)

The surface functional groups and hydrophilicity of biochar can be chemically modified to suit the specific requirements of environmental protection such as removal of contaminants from water/wastewater and soil amendment for contaminated land (Li et al.,

Table 3
The enhanced performance and mechanisms of acid/base treated and chemically oxidized biochars.

Modification	Sorbate	Sorption capacity	Enhancement	Mechanisms	Functionalities	References
H_3PO_4 KOH	N/A	N/A	Increase of water extractable organic carbon content	Hydrolysis of the ester groups formed during the pyrolysis	N/A	Lin et al. (2012)
H_2SO_4 + oxalic acids	Sulfamethazine	183 −229 L kg^{-1}	N/A	Ligand- and proton-enhanced processes; Increase in surface area by acid treatment	N/A	Vithanage et al. (2015b)
H_2SO_4 KOH	Tetracycline	23.26 mg g^{-1} 58.82 mg g^{-1}	Larger porosity and specific surface area; higher carbon and oxygen contents; lower inorganic ash content	π−π electron donor acceptor interaction between biochar surface and aromatic ring	Oxygen functional groups	Liu et al. (2012)
KOH	Cu^{2+}; Cd^{2+}	31 mg g^{-1}; 34 mg g^{-1}	About 20 times higher of sorption capacity than powered activated carbon	Electrostatic attraction, ion exchange, surface complexation, and/or surface precipitation	Aromatic carbon	Regmi et al. (2012)
KOH	As^{5+}	30.98 mg g^{-1}	More than 1.3 times higher sorption capacity		N/A	Jin et al. (2014)
NaOH	Chloramphenicol	~2100 mg kg^{-1}	Increase of surface graphitic carbon and O-containing groups	Electron-donor-acceptor π−π interaction and formation of H-bonds between N-containing group in CAP and sorbent surface	Carbonyl and carboxyl groups	Fan et al. (2010)
H_2O_2 (Oxidation)	Hg	1470.5 −1347.9 μg g^{-1}	Significantly higher sorption capacity than commercial activated carbons (380−618 ng mg^{-1})	Higher total pore volume and S_{BET} area. Surface oxygen functional groups enhance electron transfer, mercury oxidation and provide chemisorption centers	Carbonyl, carboxyl and ester groups	Tan et al. (2011)
H_2O_2 (Oxidation)	Pb^{2+}	22.82 mg g^{-1}	Sorption for Pb^{2+} was 20 times higher than unmodified biochar	Increase of carboxyl groups facilitate formation of bound complexes with Pb^{2+}	Carboxyl groups	Xue et al. (2012)
(1) H_2SO_4 + HNO_3 (2) NH_4OH + $Na_2S_2O_4$ + acetic acid (Amination)	Cu^{2+}	12.47 −15.97 mg g^{-1}	About 4.62% N was present on modified biochar; 5-fold and 8-fold enhancement of sorption capacity in batch and fixed-bed experiments, respectively	Formation of outer−sphere complexes with amino groups of the modified biochar (also ion exchange and microprecipitation)	Amino groups	Yang and Jiang (2014)

2014c; Yakout et al., 2015). Generally biochar produced at low temperature (250−400 °C) has more C═C and C−H functional groups (Novak et al., 2009). Chemical oxidation using HNO_3, $KMnO_4$, H_2O_2, H_3PO_4, or HNO_3/H_2SO_4 mixture can introduce acidic functional groups such as carboxylic, carbonyl, lactonic, and phenolic groups on the C surface at relatively low temperatures (Li et al., 2014c; Qian et al., 2015; Shafeeyan et al., 2010; Stavropoulos et al., 2008). A greater amount of O-containing functional groups was introduced by chemical modification using HNO_3 compared to $KMnO_4$, illustrating a stronger oxidizing capability of HNO_3 (Li et al.,

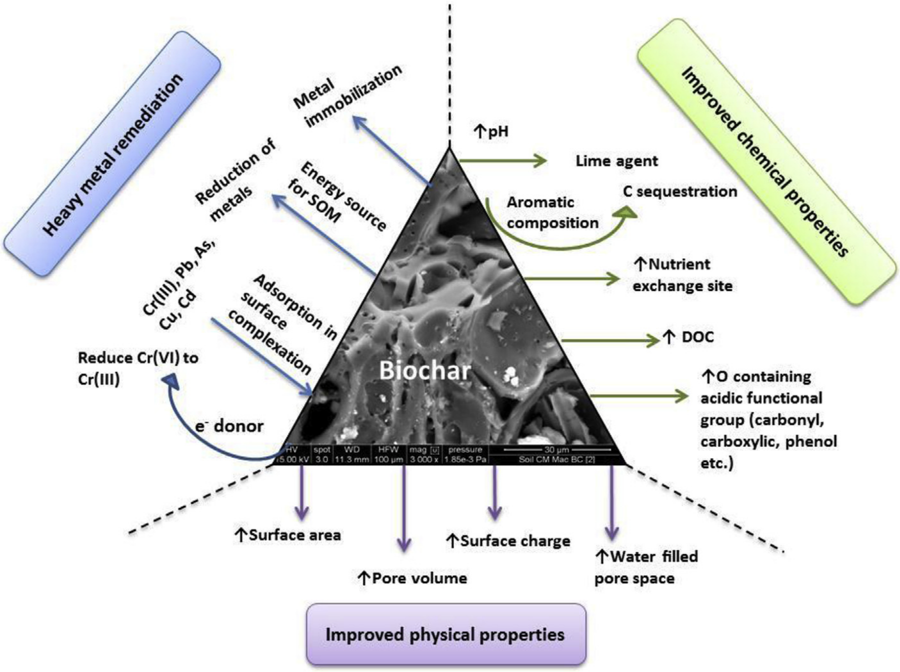

Fig. 2. Enhanced performance of engineered biochars.

2014d). Besides, H_2O_2 modification was also able to increase the carboxylic content from 2.1 to 8.2% (Tan et al., 2011) or from 16.4 to 22.3% (Xue et al., 2012) by oxidizing the carbonized surface of biochar. In view of the intrinsic oxidizing character, H_3PO_4 or H_2SO_4 also partially oxidize the C surface and enrich the carboxylic groups to some extent (Liou and Wu, 2009; Qian et al., 2015). Surface carboxylation is primarily accomplished by single-stage oxidation.

In addition to O-containing functionalities, N-containing functional groups (amide, imide, lactame, pyrrolic, and pyridinic groups) play an important role in environmental applications for their strong complexation affinities, especially for base metal cations such as Cu, Zn and Cd (Buttry et al., 1999; Shafeeyan et al., 2010). Introduction of N-containing functional groups can be attained by nitration followed by reduction on the C surface (Chingombe et al., 2005; Yang and Jiang, 2014). The dissociation of HNO_3 forms highly active intermediate nitronium ions that react with the aromatic rings and turn into nitrated products ($-NO_2$) on the biochar surface. Since the nitration of aromatic surfaces is limited by the slow rate of nitration and small quantities of NO_2^+ (Carey and Sundberg, 2007), simultaneous addition of concentrated H_2SO_4 is necessary to facilitate the formation of nitronium ions. The nitration is believed to take place via electrophilic aromatic substitution which introduces nitrogen groups on aromatic rings in biochar (Lehmann and Joseph, 2009; Yang and Jiang, 2014). The nitro-groups are subsequently reduced to amino groups on the surface by using sodium dithionite ($N_2S_2O_4$) as a reducing agent (Chingombe et al., 2005; Yang and Jiang, 2014). Surface amination results introduction of amino-groups which provide basic properties and strong affinities to pollutants.

Using chitosan (naturally abundant polysaccharide) as the modification agent, Zhou et al. (2013) introduced amine functional group on biochar surfaces to improve its sorption ability to heavy metals, like, Pb^{2+}, Cu^{2+}, and Cd^{2+}. They found that the coating of chitosan on biochar surfaces can also improve its performance as a soil amendment and concluded that chitosan-modified biochar may be used as an effective, low-cost, and environmental-friendly sorbent to remediate heavy metal contamination in the environment. The amine groups of chitosan enable enables high metal uptake due to the formation of strong chemical bonds with metal ions (Yong et al., 2013, 2012).

Hydrogen peroxide (H_2O_2) modification of peanut hull biochar surface increased O-containing functional groups, especially carboxylic group which enhances the heavy metal (Cd^{2+}, Ni^{2+} and Pb^{2+}) sorption capacity of biochar (Xue et al., 2012). Yang and Jiang (2014) reported that amino modified biochar with increased functional groups, including N—H stretching (peak around 3650 cm^{-1}), N—H bending vibration (band near 1647 cm^{-1}), C—N stretching (peak at 1394 cm^{-1}) and CH_2 and C—O stretching (peaks at 2976 and 1066 cm^{-1}) in the Fourier transform infrared (FTIR) spectra, could effectively remove Cu^{2+} from aqueous solution, because Cu^{2+} was strongly complexed with amino functional groups on biochar surface. Furthermore, biochar modified with KOH increased O-containing functional groups (O—H, C—O, C=O and COOH) and thus improved tetracycline sorption capacity (Liu et al., 2012). At neutral pH, O-containing functional groups on the surface of alkali modified biochar facilitated the formation of H_2 bonding with tetracycline molecules thus improved its sorption capacity. The H_2O_2 treated biochar has also been reported to contain high amount of O-containing functional groups and effectively removes aqueous heavy metals such as Pb^{2+}, Cu^{2+}, Ni^{2+}, and Cd^{2+} (Xue et al., 2012).

2.1.3. Treatment with organic solvents

Carboxylic group modifications can also be accomplished by using water-soluble carbodiimides and esterification via acidic methanol (Gardea-Torresdey et al., 1990). The use of acidified methanol for carboxylic modification is inexpensive. For example, rice husk biochar which has previously been treated with NaOH and subsequently modified with acidic methanol showed an increase in surface functional groups (Jing et al., 2014). The chemical reactions involved in methanol modification are esterification and then direct reaction between the carbonyl groups of biochar with methanol (Jing et al., 2014).

Methanol modified biochar was found to be rich in ester and hydroxyl groups than unmodified biochar, which facilitated the formation of electron-donor-acceptor (EDA) interaction between biochar surface and organic contaminants (contaminated soil and water, pharmaceutical manufacturing wastewater) (Jing et al., 2014). X-ray photoelectron spectroscopic (XPS) analysis revealed that electron density of O atoms on biochar surface increased by modification with methanol and displayed stronger basicity than O atoms on unmodified biochar. This was explained by strong electron-withdrawing ability of carbonyl group on the biochar surface, which can attract electrons of hydroxyl and other related groups (Jing et al., 2014).

The study conducted by Jing et al. (2014) revealed that the methanol modified biochar was more effective in tetracycline removal than unmodified biochar due to alteration of the functional groups and enrichment of O-containing groups on biochar, which might play a prominent role in tetracycline sorption. The mechanism suggested by the authors was the formation of electron donor acceptor interaction between hydroxyl group or ionized moiety (—O— acts as n-electron donors) of methanol modified biochar and the electron-depleted sites (π-electron acceptors).

2.1.4. Surfactant modifications

Surfactants are classified into cationic, anionic, nonionic, and gemini surfactant according to the nature of the hydrophilic group (Paria, 2008). While surfactants are usually used as an additive in industrial production, and washing detergents in environmental remediation, they have also been widely used in recent decades as a chemical reagent to modify the surface properties of different solid materials such as bentonite and zeolite.

In view of the negatively charged surface of biochar, cationic surfactant can easily be captured by biochar via electrostatic attraction, and exchange with abundant exchangeable cations, such as Mg^{2+}, Na^+, K^+, in biochar matrix, and subsequently a surfactant—biochar complex is formed (Erdinç et al., 2010; Saleh, 2006). For example, Saleh (2006) found that sorption of cationic surfactant cetylpyridinium chloride (CPC) on granular charcoal was mainly via ion-exchange at low concentration levels. A partial monomolecular layer may be formed with an increase of CPC concentration in solution. As further increase of CPC concentration, the hydrophobic interaction between hydrophobic chains of CPC and charcoal enhances the adsorption of CPC. Han et al. (2013) reported the effects of cationic surfactant on pentachlorophenol (PCP) sorption by activated carbon and biochar. Cationic surfactant cetyltrimethyl ammonium bromide (CTAB) was simply added in the solution containing PCP, and the modification process of biochar by CTAB occured via ion-exchange simultaneously with the sorption of PCP on biochar-CTAB complex. Thus, cationic surfactants can be used as an effective agent to modify biochar to enhance removal of anionic pollutants.

Nonionic surfactant can also be sorbed by charcoal via physisorption as indicated by low free energy changes in sorption (Santhanalakshmi and Balaji, 1996). About 300 mg g^{-1} of TX-100 was observed to be loaded on charcoal (Hamid et al., 2014). Li et al. (2014b) also found certain degree of sorption of nonionic surfactant TX-100 onto biochar. In contrast, due to electrostatic repulsion, both monomolecular and micellar anionic surfactants are not easily sorbed on the surface of biochar. For example, very weak sorption of anionic surfactants on charcoal was found by Fujita et al. (1991). However, Erdinç et al. (2010) observed a significant sorption of anionic surfactant SDS on activated charcoal.

Han et al. (2013) found that after modification of biochar with CTAB, PCP sorption capacity of biochar decreased with increasing aqueous CTAB concentrations. This may due to the hindrance of hydrophobic sorption site by CTAB sorption. On the other hand, mobilization and solubilization of PCP by CTAB in solution might also lead to the decrease of PCP sorption on biochar. The presence of cationic surfactant CTAB significantly decreased the sorption amount of amphiphilic phenothiazine drug thioridazine hydrochloride (THCl) on activated charcoal (Erdinç et al., 2010). Besides the sorption-site-hindrance mechanism, competition of cationic surfactant with cationic THCl prohibited the sorption of THCl on charcoal. However, the presence of anionic surfactant only slightly decreased THCl sorption, while nonionic surfactant TX-100 increased THCl sorption (Erdinç et al., 2010). It is believed that sorption of nonionic surfactant on charcoal was driven by physisorption with low free energy changes of sorption (Santhanalakshmi and Balaji, 1996), and THCl may be incorporated into the adsorbed nonionic surfactant during the sorption process (i.e., co-adsorption).

2.1.5. Coating of biochar

Coating of biochar with metal oxides has been recently used to improve the properties of biochar and subsequently enhance its sorption capacity (Samsuri et al., 2013; Wang et al., 2012). For example, sorption of anionic dyes by biochar is very ineffective due to the electrostatic repulsion between dye molecular and negatively charged biochar surface. Hence, coating of biochar could change surface properties of biochar.

2.1.5.1. Coating with metal oxides. Wang and colleagues synthesized cobalt (Co)- and Fe-coated bamboo charcoal for the removal of heavy metals from aqueous solution (Wang et al., 2012; Zhang et al., 2013b). Commercially available bamboo charcoal was dipped in a 100 mL solution containing cobalt nitrate [$Co(NO_3)_2.6H_2O$] or $FeCl_3$ and 9 M HNO_3, followed by heating with microwave at 640 W power and a frequency of 2.45 GHz for several minutes. Besides, magnesium hydroxide-coated wheat straw biochar was prepared using $MgCl_2$ and NaOH solution (molar ratio OH/Mg = 1.5) (Zhang et al., 2014b). The Fe-coated biochar had significantly increased hydroxyl groups compared to unmodified biochar because of the formation of iron oxides on carbon surface (Zhang et al., 2013b).

The Fe_3O_4-coated bamboo charcoal was synthesized by Zhao et al. (2013) as a sorbent for solid-phase micro-extraction to remove PBDEs in water. Ferric chloride ($FeCl_3.6H_2O$) as well as some additives, such as urea and tetrabutylammonium bromide, was prepared in solution to incorporate with bamboo, and then the residue solid was heated at 450 °C for 3 h under N_2 to obtain bamboo charcoal/Fe_3O_4 composites. Bamboo charcoal coated with Fe_3O_4 was synthesized by Zhao et al. (2013) to pre-concentrate polybrominated diphenyl ethers (PBDEs) in water for gas chromatography-mass spectrometry analysis. The Fe_3O_4 film surfaces are terminated by a hexagonal oxygen layer covered by quarter monolayer of iron cations that can form cation-π bonds (Joseph et al., 2000), indicating that for chemicals with π-electrons, such as aromatic compounds, are favored to sorb on Fe_3O_4 nanoparticles. The results showed that Fe_3O_4-coated bamboo charcoal was more effective for PBDEs concentration than other sorbents (Zhao et al., 2013). Also, Fe(III)-coated biochar was prepared using $FeCl_3$ salt. Coating the biochar with Fe(III) greatly increased As^{3+} and As^{5+} sorption capacities (Samsuri et al., 2013).

Zhang et al. (2014b) reported that the sorption capacity of MgO-coated biochar (MC) for anionic dye (directly frozen yellow, DFY) was significantly larger than that of the uncoated biochar by about 5 times. It was concluded that MC surface may be positive in solution after magnesium hydroxide coating, which enhanced the sorption of anionic DFY. Furthermore, FT-IR spectra showed that more functional groups were found on MC, which facilitated the removal of DFY.

Wang et al. (2012) reported a significant increase of Cr^{6+} oxyanion sorption by cobalt-coated bamboo charcoal (Co-BC) compared with unmodified charcoal. The Co-BC exhibited higher surface area and pore volume than unmodified charcoal, which led to the higher sorption capacity. However, nitric acid and microwave heating were also included during the production procedure of Co-BC, so it was not clear that this increment was caused only by Co^{2+}-coating or co-effect of acid and microwave treatment (Wang et al., 2012).

2.1.5.2. Coating with carbon nanotubes. Although carbon nanotubes (CNTs) are very effective for contaminant removal due to the high surface area and nanostructure, the high cost and inconvenience for engineering application limited its use. Therefore, biochar could serve as a microporous/mesoporous carrier of CNTs to develop new effective and recyclable sorbents for water and waste water treatment. For example, hybrid multi-walled CNT-coated biochar was made by dip-coating biomass into varying concentrations of carboxyl-functionalized CNT solutions (0.01% and 1% w/w) prior to slow pyrolysis (tubular furnace) at 600 °C/1 h at 10 °C min^{-1} under N_2 flow (Inyang et al., 2014). If necessary, anionic surfactant SDBS was employed to disperse CNTs in solution, and then followed the production procedure as described above (Inyang et al., 2015).

The CNTs were also grown to bamboo biochar using chemical vapor deposition (CVD), as suggested by Zhang et al. (2009). After bamboo biochar production in N_2, it was pretreated with ferrocene solution in xylene, which was fed into a CVD furnace by a peristaltic pump at a reaction temperature of 820 °C for several minutes with Ar and H_2 mixture gas flowing through the system. Similar CVD method to produce CNTs-coated bamboo biochar was suggested by Huang et al. (2012) using ferric nitrate as a catalyst.

Hybrid multi-walled CNT-coated biochar exhibited higher surface areas, porosity and thermal stability compared with uncoated biochar (Inyang et al., 2014). For example, the surface area of bagasse biochar was only 9 $m^2\ g^{-1}$, while it was 120 and 390 $m^2\ g^{-1}$ for 0.01% and 1% (w/w) CNTs loaded biochar, respectively. A significant increase of surface area and pore volume was also observed with an increase of CNTs loading on biochar Inyang et al. (2014). On the other hand, cobalt-coated bamboo biochar exhibited higher surface area and pore volume than uncoated biochar, which led to the higher Cr(VI) sorption capacity (Wang et al., 2012). Similarly, a significant increase of surface area and pore volume were also observed with the increase of Fe amount coated on bamboo charcoal (Zhang et al. (2013b).

Addition of surfactant (SDBS) for CNTs dispersion during production of CNTs-biochar composite resulted in significantly higher sorption capacity of CNTs-biochar for contaminants (sulfapyridine (SPY) and Pb^{2+}) than without SDBS due to the excellent dispersion and distribution of CNTs on biochar surface (Inyang et al., 2015). Interestingly, no obvious competition was observed between Pb^{2+} and sulfapyridine, indicating site-specific sorption of these two contaminants on CNTs-coated biochar surface (Inyang et al., 2015).

Besides contaminant sorption, hydrogen storage capacity was evaluated on multi-walled carbon nanotubes (MWCNTs) that were grown on Taiwan bamboo charcoal using microwave plasma-enhanced chemical vapor deposition. However, only a slight improvement was observed (0.52 wt.%) compared with unmodified charcoal due to lower hydrogen storage capacity of MWCNTs (0.22 wt.%) than charcoal (0.43 wt.%) (Miao et al., 2010).

As the increase of growth time of CNTs on bamboo charcoal with chemical vapor deposition approach, more CNTs incorporated with charcoal and the sorption capacity for copper increased (Saleh, 2006). Although surface area of CNTs-coated biochar decreased as increase of CNTs loading, the introduction of functional groups by chemical vapor deposition led to the enhancement of Cu sorption. Huang et al. (2012) found the similar phenomenon that surface area of CNTs-coated bamboo charcoal was much lower than the unmodified charcoal, but much more acid functional groups were found on the surface of CNTs-charcoal composites. These functional groups may easily interact with Pb^{2+} and form a stable form to immobilize it on composite surface, which enhanced the sorption capacity of Pb^{2+}.

Inyang et al. (2014) compared the methylene blue (MB) sorption capacities of unmodified hickory (HC) and bagasse biochars (BC) and CNT-biochar composites (HC-CNT and BC-CNT). The maximum sorption capacities of HC-CNT and BC-CNT (2.4 and 5.5 mg g^{-1}, respectively), were almost twice those of their respective unmodified biochar (1.3 and 2.2 mg g^{-1}, respectively). Methylene blue sorbed onto high affinity binding sites within CNT. Additionally, the biochar showed an ability to sorb methylene blue by itself when the sorption sites of CNT were filled. Electrostatic attraction was the dominant mechanism for sorption of MB and microporous diffusion controlled its sorption rate (Jing et al., 2014). The observed sorption capacities were much lower than those of some other hybrid CNT materials; however, CNT-biochar synthesis procedure is simple and inexpensive. Thus, the CNT-biochar nanocomposite can be considered as a promising, inexpensive sorbent material for removing dyes and organic pollutants from aqueous systems.

2.1.5.3. Coating with graphene. Graphene has attracted the attention of both scientists and engineers after its discovery for its special two-dimensional structure and unique properties, such as mechanical strength, surface area, thermal conductivity and electro conductivity (Chen et al., 2010). Similar to CNT, difficult separation and recovery for reuse limit the wide application of graphene in water and wastewater treatment. To overcome these disadvantages, composite of graphene covering particles are synthesized and biochar is one of the good candidates as a carrier of graphene. Synthesis of graphene-coated biochar also usually follows the two-step dip-coating procedure as above. For example, peanut shell biomass was dipped in graphene suspension to absorb graphene, and then pyrolyzed in a muffle furnace through slow pyrolysis in a N_2 environment at temperatures of 300 and 500 °C for 2 h (Ghaffar and Younis 2014). Similar coating approach was also reported by Zhang et al. (2012b) that graphene sheets were coated onto cotton wood by dipping, and then the graphene-coated biomass feedstock (milled cotton wood) was pyrolyzed in N_2 environment at 600 °C for 1 h.

Sorption enhancement of phenol and methylene blue (MB) by graphene-coated biochar was observed by Ghaffar and Younis (2014). Higher surface area and pore volume after loading of graphene on biochar may be the main reasons for increased sorption. Besides, $\pi-\pi$ bonding between graphene sheets and phenol or MB contributed to the increase of sorption amount. Zhang et al. (2012b) observed a much more significant increase of MB on graphene-coated biochar (about 20 times higher), and strong $\pi-\pi$ bonding between graphene sheet on biochar surface and MB was believed to be the predominant mechanism for the enhancement of MB sorption by graphene-coated biochar. However, no surface area data of biochar and graphene-coated biochar was available in this study, so it was not possible to account for the contribution of surface area to the sorption.

2.2. Physical modification

In general, physical/mechanical modification methods are usually simple and economically feasible, but are less effective than chemical modification methods. Physical modification process uses oxidizing agents such as carbon dioxide (CO_2), steam and air and does not involve any chemicals.

2.2.1. Steam activation

Through steam activation process, conventional biochar could potentially be upgraded to activated biochar with improved carbonaceous structures and high surface area. Steam activation is obtained when the initial pyrolysis reactions, occurring in oxygen free atmosphere at moderate temperatures (400–800 °C), are complemented by a second stage in which the resulting biochar are subjected to a partial gasification with steam. This promotes partial devolatilization and crystalline C formation in biochar (Chia et al., 2015). Steam application may change the properties of biochar by removing the trapped products of incomplete combustion during thermal treatment (Manyà, 2012). Typical reactions of the steam activation involves an initial exchange of oxygen from the water molecule to the carbon surface site C(f) to create a surface oxide C(O) and H_2 gas (Lussier et al., 1998) and the produced H_2 may react with the C surface to form surface hydrogen (H) complexes [C(H)] (Bach, 2007) (Eqs (1)–(3)). Steam oxidizes the C surface sites generating H_2 and CO_2 which may activate the surface of biochar and inhibit the gasification reaction of C sites.

$$\mathrm{C\,(f) + H_2O \rightarrow C(O) + H_2} \quad (1)$$

$$\mathrm{2C\,(f) + H_2 \rightarrow 2C(H)} \quad (2)$$

$$\mathrm{CO + H_2O \rightarrow CO_2 + H_2} \quad (3)$$

Additional syngas in biochar after pyrolysis may be liberated during steam activation process in the form of H_2 increasing the surface area and pore volume (Rajapaksha et al., 2014a, b). Hence, several studies have investigated the potential use of steam activated biochar on soil remediation and water/wastewater treatment in comparison with non-activated biochar (Table S2). Lima et al. (2010) produced steam activated biochar from waste biomass at atmospheric pressure at 800 °C for 45 min. Steam activation was accomplished by injecting water at 3 mL min^{-1} into the N_2 gas flow (0.1 m^3 h^{-1}) entering the heated retort. Samples were subsequently washed with 0.1 mol L^{-1} HCl to remove surface ash, water rinsed three times and dried overnight at 80 °C. Biochar produced by flow-through pyrolysis of tea waste and invasive plant biomass were steam activated at a flow rate of 5 mL min^{-1} for 45 min, under the peak temperature at 300 and 700 °C (Rajapaksha et al., 2015, 2014b). These biochars were directly used for the removal of veterinary antibiotics from water without any washing procedure. Only a few studies attempted to optimize steam activation parameters, of which activation time and the quantity of steam used may be crucial factors controlling the physical properties and sorption capacity of resulted biochar.

This steam activation process is known to create new porosities and enlarge diameters of smaller pores created during pyrolysis (Lima et al., 2010). A considerable increase in surface area (from 342 mg g^{-1} to 576.09 m^2 g^{-1}) was observed by steam activation of tea waste biochar (Rajapaksha et al., 2014b). This increment of surface area could be attributed to corrosion of biochar surface and release of additional syngas from the biochar, mainly in the form of hydrogen (Demirbas, 2004). Similarly, steam activation increases the pore volume of the biochar by removing the trapped products (volatile gases). Moreover, steam activation enhances the development and accessibility of internal pores in biochar (Chia et al., 2015).

It has been shown that the activation of biochar by an oxidizing agent such as steam enhances both inorganic and organic sorption capacity of conventional biochar. For instance, Rajapaksha et al. (2015, 2014a) successfully produced steam activated tea waste and invasive plant derived biochar as a promising remedy of veterinary antibiotics removal from water. The steam activated invasive plant derived biochar produced at 700 °C showed 55% increase in sorption capacity compared to that of non-activated biochar produced at the same temperature (Rajapaksha et al., 2015). The steam activation process increases the sorption capacity by increasing the surface area of the biochar.

2.2.2. Gas purging

Modification of biochar with high temperature CO_2-ammonia mixture treatment has been investigated to adsorb gases (CO_2) (Xiong et al., 2013; Zhang et al., 2014b). Xiong et al. (2013) produced CO_2 and NH_3 modified biochar under the a range of production temperatures. After the production of cotton stalk biochar, it was gradually heated up to preset temperature (500–900 °C) in a quartz reactor with N_2 purging and then CO_2 or NH_3 was purged. The ammonification (introduction of NH_3) could introduce N-containing groups onto the biochar and increase N content up to 3.91 wt.% in CO_2-ammonia modified biochar, whereas CO_2 treatment could play significant role in pore formation and improve the microporous structure of biochar facilitating gas sorption capacities of biochar (Xiong et al., 2013).

Xiong et al. (2013) showed that the surface area and pore volume of CO_2-modified biochar was much higher than unmodified biochar. Carbon dioxide could react with C of the biochar sample to form CO (i.e., hot corrosion), thereby creating microporous structures. The clay-biochar composites produced from biomass mixture with kaolinite and montmorillonite exhibited lower surface areas compared to unmodified biochar. This may be due to blockage of pores in biochar by clay minerals (Yao et al., 2014).

At ambient temperature, gas sorption capacity of CO_2 modified biochar was significantly higher than that of the unmodified biochar (Xiong et al., 2013). Sorption capacity of modified biochar showed linear relationship with the micropore volume and the mechanism of CO_2 sorption was identified as physical sorption (Xiong et al., 2013).

2.3. Impregnation with mineral oxides

As a new concept, engineered biochar has been prepared by impregnation of minerals with biochar (Yao et al., 2014, 2011a, 2011b; Zhang et al., 2012a). Clay minerals have been extensively used for contaminant removal in view of their composition, cation exchange capacity (CEC), surface charge and mineralogical structure. Montmorillonite, gibbsite, and kaolinite are among the most commonly used clay minerals, as well as iron oxides, as low-cost sorbents (Goldberg et al., 1996; Manning and Goldberg, 1996; Murray, 1991; Rajapaksha et al., 2012; Vithanage et al., 2006). Yao et al. (2014) distributed clay particles within the biochar matrix to enhance its functionality. The clay (montmorillonite and/or kaolin) were mixed with biomass (bamboo, bagasse, and hickory chips) and pyrolyzed in a N_2 environment at 600 °C for 1 h. In these biochar-clay composites, biochar act as a good porous structure to support and host the distribution of the fine clay particles within the matrix. In another study, thermal pyrolysis of $AlCl_3$ pretreated biomass produced biochar/AlOOH composite with robust interconnected three-dimensional biochar network. In this process, biochar networks prevented particle aggregation and created nanosized AlOOH on C surfaces with uniform morphology and homogeneous distribution (Zhang and Gao, 2013).

Anaerobically digested biomass, $MgCl_2$-pretreated biomass and Mg-rich biomass have been recently investigated to produce engineered Mg-biochar nanocomposites by pyrolysis (Yao et al., 2014, 2011a). The engineered Mg-biochar nanocomposites were prepared through pyrolyzing anaerobically digested Mg-rich biomass residues (Yao et al., 2011a). Zhang et al. (2012a) synthesized porous MgO-biochar nanocomposites with 20-nm-thick flakes of polycrystalline MgO from different feedstock materials (sugar beet tailings, sugarcane bagasse, cottonwoods, pine woods, and peanut shells). The feedstocks were immersed in $MgCl_2$ solutions, and the resulted dry-mixture of $MgCl_2$ incorporated biomass was heated at 10 °C min^{-1} at 600 °C under N_2 flow for 1 h. Application of N_2 treatment is essential to remove by-product gases including HCl and thereby facilitating the formation of MgO particles in the biochar matrix. In addition, direct use of Mg/Ca enriched tomato tissues is another innovative approach of producing Mg-enriched biochar (Yao et al., 2013b) which contains nanosized MgO and $Mg(OH)_2$ particles within the biochar matrix.

Also, Mn oxide-modified pine biochar and birnessite-modified biochar were prepared by two modification methods for the purpose of improving sorption ability for As^{3+} and Pb^{2+} (Wang et al., 2015a). Pre-soaking pine wood biomass in $MnCl_2.4H_2O$ solution and subsequent pyrolysis yielded Mn-oxide modified biochar, whereas birnessite modified biochar was produced by impregnation of pine wood biochar with birnessite via precipitation following pyrolysis (Wang et al., 2015a).

Composites of manganese oxides (MnOx) with different phases, i.e., β-MnO_2, δ-MnO_2, and MnO_2-coated sand, were reported to have strong binding capacities with heavy metals (Tripathy and Kanungo, 2005) and phosphates (Park et al., 2015b). Therefore, Song et al. (2014) have attempted to combine the advantages of MnOx and biochar into new engineered biochar composites with enhanced functions. A series of MnOx-loaded biochars with different MnOx coverage (2.5, 10, and 60%) were prepared via $KMnO_4$ modification of corn straw biochar under high temperature (600 °C). Layered structures of micro/nano-MnOx were well dispersed on the biochar surface that was thermally treated with 10% $KMnO_4$, and the oxidation states of Mn was found as Mn^{3+} and Mn^{4+} (Song et al., 2014).

The $KMnO_4$ addition to biochar greatly changed surface area and pore volumes of biochar. A considerable decrease in surface area (61.0–2.28 m^2 g^{-1}) was observed, whereas average pore width increased from 23.7 to 92.2 nm with increasing $KMnO_4$ loading (Song et al., 2014). These structural changes of MnO_x-biochar composites may be due to destruction of nanopore structures and deformation from nanopores into meso-/macropores by $KMnO_4$ which normally acts as a strong oxidizing agent (Song et al., 2014). Similarly, Fe-impregnated biochar prepared though hydrolyzes iron salt onto hickory biochar had lower surface areas than untreated biochars (Hu et al., 2015).

Using FTIR data, Song et al., 2014 have showed noticeable increase of O-containing functional groups in MnOx-biochar composites. Similarly, the majority of surface oxygen in MnO_x loaded biochar composites were bonded to Mn in the form of Mn–O (63.9%) and Mn–OH (26.3%). The XPS analysis confirmed the presence of manganese oxide (Mn–O), hydroxyl bonding to Mn (Mn–OH), hydroxyl on carbonaceous surface (C–OH), as well as chemisorbed water on biochar surfaces.

Modification induced changes in the elemental composition of biochars are listed in Table 4. Biochar modified with montmorillonite and kaolinite significantly increased the biochars' aluminum and iron content compared to that of unmodified biochar, whereas

Table 4
Characteristics of modified biochars produced from different treatments.

Treatment	Feedstock	Modified/unmodified	Pyrolysis temperature	Ash	pH	C	H	O	N	Surface area	Pore volume	Reference
			°C	%		%	%	%	%	$m^2 g^{-1}$	$cm^3 g^{-1}$	
H_2O_2 modification	Peanut hull	Unmodified	300	–	6.2	56.3	5.6	36.6	0.9	N_2: 1.3 CO_2: 96.9	–	Xue et al. (2012)
		Modified		–	4.4	48.3	5.8	43.8	0.8	N_2: 1.4 CO_2: 114.4	–	
KOH modification	Rice husk	Unmodified	450–500	42.2	7.0	42.1	2.2	0.5	12.1	34.4	0.028	Liu et al. (2012)
		Modified		3.5	7.0	76.4	3.3	0.9	16.9	117.8	0.073	
Methanol modified biochar	Rice husk	Unmodified	450	1.0	–	70.6	3.5	24.1	0.8	51.9	0.031	Jing et al. (2014)
		Modified		0.9	–	71.3	3.6	23.4	0.8	66.0	0.051	
Amino modified biochar	Saw dust char	Unmodified	500	–	<4	68.7	3.8	–	0.3	2.6	0.005	Yang and Jiang (2014)
		Modified		–	>6	62.1	4.2	–	4.6	2.5	0.005	
$FeCl_3(FeCl_3.6H_2O)$ modified biochar	Wheat straw	Unmodified	450	–	7.0	47.2	2.4	18.4	1.1	9.5	0.012	Li et al. (2014c)
		Modified		–	8.3	25.9	1.7	21.6	0.6	50.0	0.038	
Zn-loaded biochar	Pine cone	Unmodified	500	2.1	–	67.9	3.9	22.1	0.5	6.6	0.016	Van Vinh et al. (2015)
		Modified		2.1	–	71.2	3.0	20.4	0.5	11.5	0.028	
Steam activated biochar	Tea waste	Unmodified	300	5.7	7.9	70.1	5.2	19.6	5.0	2.3	0.006	Rajapaksha et al. (2014b)
		Modified		6.4	8.6	71.5	4.8	18.2	5.5	1.5	0.004	
Steam activated biochar	Tea waste	Unmodified	700	10.9	11.0	85.1	2.0	8.9	3.9	342.2	0.022	Rajapaksha et al. (2014b)
		Modified		16.7	10.5	82.4	2.1	11.6	3.9	576.1	0.109	
Steam activated biochar	Invasive plant (*Sicyos angulatus* L.)	Unmodified	300	25.4	10.9	66.0	5.6	23.1	5.1	0.9	0.004	Rajapaksha et al. (2015)
		Modified		28.7	11.1	68.1	5.1	21.4	5.1	1.2	0.003	
Steam activated biochar	Invasive plant (*Sicyos angulatus* L.)	Unmodified	700	43.7	12.3	69.4	1.3	24.4	4.6	2.3	0.008	Rajapaksha et al. (2015)
		Modified		70.7	11.7	50.6	1.7	44.9	2.5	7.1	0.038	
CO_2-ammonia modified biochar	Cotton stalk	Unmodified	600	–	–	–	–	–	1.1	224.0	0.070	Zhang et al. (2014a)
		Modified		–	–	–	–	–	1.0	351.0	0.130	
Clay-biochar composites	Bamboo	Unmodified	600	–	–	80.9	2.4	14.9	0.1	375.5	–	Yao et al. (2014)
		Modified (montmorilinite)		–	–	83.3	2.3	12.4	0.2	408.1	–	
		Modified (kaolinite)		–	–	81.0	2.1	15.8	0.2	239.8	–	
Clay-biochar composites	Bagasse	Unmodified	600	–	–	76.4	2.9	18.3	0.8	388.3	–	Yao et al. (2014)
		Modified (montmorilinite)		–	–	75.3	2.2	18.9	0.7	407.0	–	
		Modified (kaolinite)		–	–	70.2	2.4	24.4	0.7	328.6	–	
Clay-biochar composites	hickory chips	Unmodified	600	–	–	81.8	2.2	14.0	0.7	401.0		Yao et al. (2014)
		Modified (montmorilinite)		–	–	80.9	2.2	15.1	0.3	376.1	–	
		Modified (kaolinite)		–	–	78.1	2.1	18.1	0.3	224.5	–	
MnOx-loaded biochar	Corn straw	Unmodified	600	5.0	–	85.3	1.7	5.2	0.8	61.0	0.036	Song et al. (2014)
		Modified (10% $KMnO_4$)		13.1	–	73.0	0.3	10.9	0.7	3.2	0.006	
		Modified (zero-valent iron)	700	–	–	–	–	–	–	101.2	0.079	
Manganese oxide-modified biochar	Pine wood	Unmodified	600	4.0	–	85.7	2.1	11.2	0.3	209.6	0.003	Wang et al. (2015a)
		Modified (Mn oxide)		14.0	–	80.0	1.9	14.6	0.3	463.1	0.022	
		Modified (birnessite)		33.4	–	61.5	1.9	27.6	0.2	67.4	0.066	
Manganese oxide modification	Peeled pine wood	Unmodified	700	–	4.5	–	–	–	–	369	0.200	Wang et al. (2014)
		Modified		–	ND	–	–	–	–	361.0	0.194	
Metal impregnated activated carbon	pulverized sub-bituminous coal	Unmodified	600 and 1000	–	6.4	81.6	–	17.9	–	190.0	0.079	Dastgheib et al. (2014)
		Modified		–	ND	65.5	–	13.2	–	245.0	0.126	
NH_3/CO_2 modification	Cotton stalks	Unmodified	600	–	–	–	–	–	1.1	224.1	0.070	Xiong et al. (2013)
		Modified		–	–	–	–	–	3.5 and 1.0	251.9 and 351.5	0.080 and 0.130	
Ca–Mg loaded biochar	Corncob	Unmodified	300, 450 and 600	4.0	–	35.5	6.3	–	0.7	ND	–	Fang et al. (2015)
		Modified		5.0	–	43.3	5.0	–	0.6	378.0	–	
$Zn(NO_3)_2$ loaded biochar	Pine cones	Unmodified	500	2.1	4.7	67.9	3.9	22.1	0.5	6.6	0.016	Van Vinh et al. (2015)
		Modified		2.1	4.0	71.2	3.0	20.4	0.5	11.5	0.028	
Magnetic biochar	Orange peel	Unmodified	250	3.1	–	56.5	5.1	–	1.7	51.6	0.059	Chen et al. (2011)
		Modified (magnetite-Fe^{3+}/Fe^{2+})		42.4	–	35.1	3.6	–	1.1	41.2	0.052	
Magnetic biochar	Orange peel	Unmodified	400	6.9	–	65.7	3.5	–	1.80	28.1	0.041	Chen et al. (2011)
		Modified (magnetite-Fe^{3+}/Fe^{2+})		35.0	–	29.4	2.2	–	0.5	23.4	0.042	
Magnetic biochar	Orange peel	Unmodified	700	14.9	–	67.0	1.5	–	2.0	501.0	0.390	Chen et al. (2011)
		Modified (magnetite-Fe^{3+}/Fe^{2+})		95.7	–	0.4	0.2	–	0.2	19.4	0.033	
Magnetic biochar	Paper mill Sludge	Unmodified	700	–	–	–	–	–	–	67.0	0.083	Devi and Saroha (2014)
		Modified (zero-valent iron)		–	–	–	–	–	–	101.2	0.079	

the C, H, N, S and O contents were relatively comparable with unmodified biochar (Yao et al., 2014). By contrast, the surface O content of MnOx-biochar composites (40.1%) was significantly higher than that of unmodified biochar (15.3%), indicating the enhancement of O-containing functional groups (Song et al., 2014).

Biochar is considered to be the most thermally stable form amongst carbon-based materials including black carbon and activated carbon and hence any negative impact on its thermal stability due to modification is likely to impact its long term application. Thermogravimetric analysis (TGA) of clay-biochar composites showed that the clay biochar-composites had similar and comparable thermal stability to that of the unmodified biochar samples (Yao et al., 2014). This suggests that the clay pretreatment of biomass precursors does not affect thermal stability of biochar. On the contrary, Inyang et al. (2014) found that biochar exhibited a higher thermal stability with an increasing introduction of CNTs, likely because of the coating of the CNTs on carbon surface. Manganese oxide modified biochar has higher thermal stability than unmodified biochar, due to the transition of Mn-oxides during the heating process (Wang et al., 2015b). However, there is insufficient information to compare the thermal stability of different types of modified biochars.

The Mg-biochar nanocomposites synthesized by Mg-enriched plant tissues were found to be a strong sorbent for P in aqueous media (Yao et al., 2013b). Also, the maximum P sorption capacities of the Mg-biochar nanocomposites synthesized through pyrolyzing anaerobically digested sugar beet tailings (Yao et al., 2011a) and $MgCl_2$-pretreated agricultural residues (Zhang et al., 2012a) were extremely higher (>100 mg g^{-1}) than that of any other carbon-based sorbents (<20 mg g^{-1}) (Biswas et al., 2007; Chouyyok et al., 2010; Yan et al., 2010). The surfaces of Mg-biochar composites have more $MgO/Mg(OH)_2$, suggesting a strong interactions between P and surface $MgO/MgOH_2$ sites. The points of zero charges of $MgOH_2$ and MgO are higher than 12 and hence the surfaces of Mg-biochar composites may be positively charged in most natural aqueous solutions with < pH 7 which facilitates electrostatic interactions between negatively charged P and biochar surfaces (Yao et al., 2011b; Zhang et al., 2012a). Enhancement of P removal by Mg-biochar nanocomposites is attributed to the presence of nanosized MgO and $Mg(OH)_2$ within the matrix and surface charge alteration of biochar (Yao et al., 2013b, 2011b). However, the impregnation of $Fe(OH)_3$ onto the Mg-biochar reduced its P sorption ability possibly due to precipitation of $Fe(OH)_3$ onto the biochar surface which covers the colloidal and nano-sized MgO particles (periclase) (Yao et al., 2011a).

The MnO_x-loaded BCs exhibited much higher sorption capacity to Cu^{2+} (160 mg g^{-1}), which is more than 8 times of the unmodified biochar (19.6 mg g^{-1}) (Song et al., 2014). Formation of inner—sphere complexes with MnO_x and O-containing groups, cation-exchange and cation-π bonding are the main mechanisms involved in increase sorption of Cu^{2+} on the MnO_x-loaded biochar (Song et al., 2014).

2.4. Magnetic modification

The multi-functional characteristics of biochar show its potential as an effective sorbent for contaminants in water and wastewater. However, powdered biochar is difficult to be separated from the aqueous matrix which makes practically unattractive for the users. Therefore, several attempts have been made to produce magnetic biochar sorbents to facilitate better separation of biochar particles after treatment process (Chen et al., 2011; Mohan et al., 2014a; Wang et al., 2015b; Zhang et al., 2013a). As the surfaces of biochars are mostly net negatively charged; therefore sorption of anionic contaminants is relatively low (Beesley and Marmiroli, 2011; Mukherjee et al., 2011) and thus engineered biochar has been produced by magnetic modification process to enhance its sorption of anionic contaminants (Chen et al., 2011; Wang et al., 2015b).

A novel, one-step method combining iron oxide and biochar formation in one-step has been proposed by Chen et al. (2011) in order to reduce the cost of the traditional loading-process of magnetic medium to biochar. This magnetic biochar was prepared by chemical co-precipitation of Fe^{3+}/Fe^{2+} on orange peel powder and subsequently pyrolyzing under different temperatures (250, 400 and 700 °C), which resulted in iron oxide magnetite formation and biochar preparation in a single step.

The surface areas of magnetic biochar prepared by chemical co-precipitation of Fe^{3+}/Fe^{2+} was smaller than the corresponding non-magnetic biochar, whereas the average pore diameter of the magnetic biochar was larger than that of non-magnetic biochar (Chen et al., 2011). This is probably because magnetic biochar contained considerable proportion of iron oxide, which have small surface areas and abundant transitional pores (2–50 nm) (Chen et al., 2011).

The hybrid sorption property of this magnetic biochar facilitates effective removal of organic pollutants and phosphate simultaneously. The presence and stability of magnetic medium in the magnetic biochar for a long time confirmed the possibility of magnetic separation after use, which is a major advantage for practical wastewater treatment process. Similarly, Zhang et al. (2013a) developed a magnetic biochar through thermal pyrolysis of $FeCl_3$ treated biomass at 600 °C. The resulting engineered biochar has colloidal or nanosized γ-Fe_2O_3 particles embedded in porous biochar matrix and thus exhibited excellent ferromagnetic property with a saturation magnetization of 69.2 emu/g (Zhang et al., 2013a), which was comparable to that of pure γ-Fe_2O_3 (76.0 emu/g). In addition, batch sorption experimental results showed that the magnetic biochar has strong sorption ability to As^{3+} in solution. Because of its ferromagnetic property, the exhausted/spent biochar can be easily separated and collected by magnetic separation.

3. Conclusions and future perspectives

The present review highlights the need of engineered biochar for contaminant removal. Modification of biochar using various techniques is likely to result in changes in its surface properties including surface area, surface charge, functional groups, and pore volume and distribution. In most cases, the clay-biochar composites exhibit lower surface areas compared to unmodified biochar due to blockage of pores by clay particles. However, the integrated performance of biochar and clay towards contaminant removal has significant increase of contaminant sorption and hence decreasing surface area does not lead to decrease of sorption performance.

Many studies have reported the importance of chemical activation process as an appealing strategy to enhance biochar's sorption ability for both organic and inorganic contaminants. However, special care has to be taken to minimize the effect of modification on stability of biochar to avoid the environmental contamination resulting from the physical/chemical activation processes. Magnetic modification method provides better solution for practical separation and recovery problems of non-magnetic sorbents. Very little information is available regarding the large scale production of engineered biochar. Therefore further investigations would be crucial to testify the applications of engineered biochar in field.

Acknowledgments

This study was supported by the National Research Foundation of Korea (NRF-2015R1A2A2A11001432) and Hong Kong Research Grants Council (Project number PolyU 152221/15E).

Appendix A. Supplementary data

Supplementary data related to this article can be found at http://

dx.doi.org/10.1016/j.chemosphere.2016.01.043.

References

Agrafioti, E., Kalderis, D., Diamadopoulos, E., 2014. Ca and Fe modified biochars as adsorbents of arsenic and chromium in aqueous solutions. J. Environ. Manag. 146, 444–450.

Ahmad, M., Lee, S.S., Lim, J.E., Lee, S.E., Cho, J.S., Moon, D.H., Hashimoto, Y., Ok, Y.S., 2014. Speciation and phytoavailability of lead and antimony in a small arms range soil amended with mussel shell, cow bone and biochar: EXAFS spectroscopy and chemical extractions. Chemosphere 95, 433–441.

Azargohar, R., Dalai, A.K., 2008. Steam and KOH activation of biochar: experimental and modeling studies. Microporous Mesoporous Mater. 110, 413–421.

Bach, M.T., 2007. Impact of Surface Chemistry on Adsorption: Tailoring of Activated Carbon. University of Florida, p. 132.

Basta, A.H., Fierro, V., El-Saied, H., Celzard, A., 2009. 2-Steps KOH activation of rice straw: an efficient method for preparing high-performance activated carbons. Bioresour. Technol. 100, 3941–3947.

Beesley, L., Marmiroli, M., 2011. The immobilisation and retention of soluble arsenic, cadmium and zinc by biochar. Environ. Pollut. 159, 474–480.

Biswas, B.K., Inoue, K., Ghimire, K.N., Ohta, S., Harada, H., Ohto, K., Kawakita, H., 2007. The adsorption of phosphate from an aquatic environment using metal-loaded orange waste. J. Colloid Interface Sci. 312, 214–223.

Buttry, D.A., Peng, J.C.M., Donnet, J.-B., Rebouillat, S., 1999. Immobilization of amines at carbon fiber surfaces. Carbon 37, 1929–1940.

Carey, F.A., Sundberg, R.J., 2007. Advanced Organic Chemistry Part B: Reactions and Synthesis. Springer, US.

Cazetta, A.L., Vargas, A.M.M., Nogami, E.M., Kunita, M.H., Guilherme, M.R., Martins, A.C., Silva, T.L., Moraes, J.C.G., Almeida, V.C., 2011. NaOH-activated carbon of high surface area produced from coconut shell: kinetics and equilibrium studies from the methylene blue adsorption. Chem. Eng. J. 174, 117–125.

Chan, K.Y., Van Zwieten, L., Meszaros, I., Downie, A., Joseph, S., 2007. Agronomic values of greenwaste biochar as a soil amendment. Soil Res. 45, 629–634.

Chan, K.Y., Van Zwieten, L., Meszaros, I., Downie, A., Joseph, S., 2008. Using poultry litter biochars as soil amendments. Soil Res. 46, 437–444.

Chen, B., Chen, Z., Lv, S., 2011. A novel magnetic biochar efficiently sorbs organic pollutants and phosphate. Bioresour. Technol. 102, 716–723.

Chen, D., Tang, L., Li, J., 2010. Graphene-based materials in electrochemistry. Chem. Soc. Rev. 39, 3157–3180.

Chia, C.H., Downie, A., Munroe, P., 2015. Characteristics of Biochar: Physical and Structural Properties. In: Biochar for Environmental Management: Science. Technology and Implementation, p. 89.

Chingombe, P., Saha, B., Wakeman, R.J., 2005. Surface modification and characterisation of a coal-based activated carbon. Carbon 43, 3132–3143.

Cho, H.-H., Wepasnick, K., Smith, B.A., Bangash, F.K., Fairbrother, D.H., Ball, W.P., 2010. Sorption of aqueous Zn[II] and Cd[II] by multiwall carbon nanotubes: the relative roles of oxygen-containing functional groups and graphenic carbon. Langmuir 26, 967–981.

Chouyyok, W., Wiacek, R.J., Pattamakomsan, K., Sangvanich, T., Grudzien, R.M., Fryxell, G.E., Yantasee, W., 2010. Phosphate removal by anion binding on functionalized nanoporous sorbents. Environ. Sci. Technol. 44, 3073–3078.

Dastgheib, S.A., Ren, J., Rostam-Abadi, M., Chang, R., 2014. Preparation of functionalized and metal-impregnated activated carbon by a single-step activation method. Appl. Surf. Sci. 290, 92–101.

Demirbas, A., 2004. Effects of temperature and particle size on bio-char yield from pyrolysis of agricultural residues. J. Anal. Appl. Pyrolysis 72, 243–248.

Devi, P., Saroha, A.K., 2014. Synthesis of the magnetic biochar composites for use as an adsorbent for the removal of pentachlorophenol from the effluent. Bioresour. Technol. 169, 525–531.

Erdinç, N., Göktürk, S., Tunçay, M., 2010. A study on the adsorption characteristics of an amphiphilic phenothiazine drug on activated charcoal in the presence of surfactants. Colloids Surf. B Biointerfaces 75, 194–203.

Fan, Y., Wang, B., Yuan, S., Wu, X., Chen, J., Wang, L., 2010. Adsorptive removal of chloramphenicol from wastewater by NaOH modified bamboo charcoal. Bioresour. Technol. 101, 7661–7664.

Fang, C., Zhang, T., Li, P., Jiang, R.-f., Wang, Y.-c, 2014. Application of magnesium modified corn biochar for phosphorus removal and recovery from swine wastewater. Int. J. Environ. Res. Public Health 11, 9217–9237.

Fang, C., Zhang, T., Li, P., Jiang, R., Wu, S., Nie, H., Wang, Y., 2015. Phosphorus recovery from biogas fermentation liquid by Ca–Mg loaded biochar. J. Environ. Sci. China 29, 106–114.

Fierro, V., Muñiz, G., Basta, A.H., El-Saied, H., Celzard, A., 2010. Rice straw as precursor of activated carbons: activation with ortho-phosphoric acid. J. Hazard. Mater. 181, 27–34.

Fujita, I., Tomooka, J., Sugimura, T., 1991. Sorption of anionic surfactants with wood charcoal. Bull. Chem. Soc. Jpn. 64, 738–740.

Fungo, B., Guerena, D., Thiongo, M., Lehmann, J., Neufeldt, H., Kalbitz, K., 2014. N_2O and CH_4 emission from soil amended with steam-activated biochar. J. Plant Nutr. Soil Sci. 177, 34–38.

Gardea-Torresdey, J.L., Becker-Hapak, M.K., Hosea, J.M., Darnall, D.W., 1990. Effect of chemical modification of algal carboxyl groups on metal ion binding. Environ. Sci. Technol. 24, 1372–1378.

Ghaffar, A., Younis, M.N., 2014. Adsorption of organic chemicals on graphene coated biochars and its environmental implications. Green Process Synth. 3, 479–487.

Glaser, Bruno, Lehmann, Johannes, Zech, Wolfgang, 2002. Ameliorating Physical and Chemical Properties of Highly Weathered Soils in the Tropics with Charcoal: a Review. Springer, Berlin, Allemagne.

Goldberg, S., Forster, H.S., Godfrey, C.L., 1996. Molybdenum adsorption on oxides, clay minerals, and soils. Soil Sci. Soc. Am. J. 60, 425–432.

Guan, X., Zhou, J., Ma, N., Chen, X., Gao, J., Zhang, R., 2014. Studies on modified conditions of biochar and the mechanism for fluoride removal. Desalination Water Treat. 1–8.

Guo, J., Xu, W.S., Chen, Y.L., Lua, A.C., 2005. Adsorption of NH_3 onto activated carbon prepared from palm shells impregnated with H_2SO_4. J. Colloid Interface Sci. 281, 285–290.

Guo, Y., Rockstraw, D.A., 2007. Activated carbons prepared from rice hull by one-step phosphoric acid activation. Microporous Mesoporous Mater. 100, 12–19.

Hamid, S., Chowdhury, Z., Zain, S., 2014. Base catalytic approach: a promising technique for the activation of biochar for equilibrium sorption studies of copper, Cu(II) ions in single solute system. Materials 7, 2815–2832.

Han, D., Liu, X.T., Zhang, G.X., 2013. Effect of cationic surfactant on pentachlorophenol sorption by sediment, active carbon and biochar. Fresenius Environ. Bull. 22, 1280–1286.

Hu, X., Ding, Z., Zimmerman, A.R., Wang, S., Gao, B., 2015. Batch and column sorption of arsenic onto iron-impregnated biochar synthesized through hydrolysis. Water Res. 68, 206–216.

Huang, Z.-H., Zhang, F., Wang, M.-X., Lv, R., Kang, F., 2012. Growth of carbon nanotubes on low-cost bamboo charcoal for Pb(II) removal from aqueous solution. Chem. Eng. J. 184, 193–197.

Inyang, M., Gao, B., Zimmerman, A., Zhang, M., Chen, H., 2014. Synthesis, characterization, and dye sorption ability of carbon nanotube–biochar nanocomposites. Chem. Eng. J. 236, 39–46.

Inyang, M., Gao, B., Zimmerman, A., Zhou, Y., Cao, X., 2015. Sorption and cosorption of lead and sulfapyridine on carbon nanotube-modified biochars. Environ. Sci. Pollut. Res. 22, 1868–1876.

Jin, H., Capareda, S., Chang, Z., Gao, J., Xu, Y., Zhang, J., 2014. Biochar pyrolytically produced from municipal solid wastes for aqueous As(V) removal: adsorption property and its improvement with KOH activation. Bioresour. Technol. 169, 622–629.

Jing, X.-R., Wang, Y.-Y., Liu, W.-J., Wang, Y.-K., Jiang, H., 2014. Enhanced adsorption performance of tetracycline in aqueous solutions by methanol-modified biochar. Chem. Eng. J. 248, 168–174.

Joseph, Y., Wuhn, M., Niklewski, A., Ranke, W., Weiss, W., Woll, C., Schlogl, R., 2000. Interaction of ethylbenzene and styrene with iron oxide model catalyst films at low coverages: a NEXAFS study. Phys. Chem. Chem. Phys. 2, 5314–5319.

Jung, C., Boateng, L.K., Flora, J.R.V., Oh, J., Braswell, M.C., Son, A., Yoon, Y., 2015. Competitive adsorption of selected non-steroidal anti-inflammatory drugs on activated biochars: experimental and molecular modeling study. Chem. Eng. J. 264, 1–9.

Kasparbauer, R.D., 2009. The Effects of Biomass Pretreatments on the Products of Fast Pyrolysis. Iowa State University.

Klijanienko, A., Lorenc-Grabowska, E., Gryglewicz, G., 2008. Development of mesoporosity during phosphoric acid activation of wood in steam atmosphere. Bioresour. Technol. 99, 7208–7214.

Kuzyakov, Y., Subbotina, I., Chen, H., Bogomolova, I., Xu, X., 2009. Black carbon decomposition and incorporation into soil microbial biomass estimated by 14C labeling. Soil Biol. Biochem. 41, 210–219.

Lehmann, J., Joseph, S., 2009. Biochar for Environmental Management: Science and Technology. Earthscan *Press*, ISBN 978-1-84407-658-1.

Li, F., Cao, X., Zhao, L., Wang, J., Ding, Z., 2014a. Effects of mineral additives on biochar formation: carbon retention, stability, and properties. Environ. Sci. Technol. 48, 11211–11217.

Li, H., Qu, R., Li, C., Guo, W., Han, X., He, F., Ma, Y., Xing, B., 2014b. Selective removal of polycyclic aromatic hydrocarbons (PAHs) from soil washing effluents using biochars produced at different pyrolytic temperatures. Bioresour. Technol. 163, 193–198.

Li, J.-h., Lv, G.-h., Bai, W.-b., Liu, Q., Zhang, Y.-c., Song, J.-q, 2014c. Modification and use of biochar from wheat straw (Triticum aestivum L.) for nitrate and phosphate removal from water. Desalination Water Treat. 1–13.

Li, Y., Shao, J., Wang, X., Deng, Y., Yang, H., Chen, H., 2014d. Characterization of modified biochars derived from bamboo pyrolysis and their utilization for target component (Furfural) adsorption. Energy & Fuels 28, 5119–5127.

Li, Y., Wang, X., Zhu, Y., Wang, L., Wang, Z., 2012. In situ preparation of biochar coated silica material from rice husk. Colloids Surf. A Physicochem. Eng. Aspects 395, 157–160.

Lima, I.M., Boateng, A.A., Klasson, K.T., 2010. Physicochemical and adsorptive properties of fast-pyrolysis bio-chars and their steam activated counterparts. J. Chem. Technol. Biotechnol. 85, 1515–1521.

Lin, Y., Munroe, P., Joseph, S., Henderson, R., Ziolkowski, A., 2012. Water extractable organic carbon in untreated and chemical treated biochars. Chemosphere 87, 151–157.

Liou, T.-H., Wu, S.-J., 2009. Characteristics of microporous/mesoporous carbons prepared from rice husk under base- and acid-treated conditions. J. Hazard. Mater. 171, 693–703.

Liu, P., Liu, W.-J., Jiang, H., Chen, J.-J., Li, W.-W., Yu, H.-Q., 2012. Modification of biochar derived from fast pyrolysis of biomass and its application in removal of tetracycline from aqueous solution. Bioresour. Technol. 121, 235–240.

Lussier, M.G., Zhang, Z., Miller, D.J., 1998. Characterizing rate inhibition in steam/hydrogen gasification via analysis of adsorbed hydrogen. Carbon 36, 1361–1369.

Ma, Y., Liu, W.-J., Zhang, N., Li, Y.-S., Jiang, H., Sheng, G.-P., 2014. Polyethylenimine modified biochar adsorbent for hexavalent chromium removal from the aqueous solution. Bioresour. Technol. 169, 403–408.

Manning, B.A., Goldberg, S., 1996. Modeling competitive adsorption of arsenate with phosphate and molybdate on oxide minerals. Soil Sci. Soc. Am. J. 60, 121–131.

Manyà, J.J., 2012. Pyrolysis for biochar purposes: a review to establish current knowledge gaps and research needs. Environ. Sci. Technol. 46, 7939–7954.

Mao, H., Zhou, D., Hashisho, Z., Wang, S., Chen, H., Wang, H.H., 2014. Preparation of pinewood-and wheat straw-based activated carbon via a microwave-assisted potassium hydroxide treatment and an analysis of the effects of the microwave activation conditions. BioResources 10, 809–821.

Miao, H.-Y., Chen, G.R., Chen, D.Y., Lue, J.T., Yu, M.S., 2010. Hydrogen storage: a comparison of hydrogen uptake values in carbon nanotubes and modified charcoals. Eur. Phys. J. Appl. Phys. 52 (null-null).

Mohan, D., Kumar, H., Sarswat, A., Alexandre-Franco, M., Pittman Jr., C.U., 2014a. Cadmium and lead remediation using magnetic oak wood and oak bark fast pyrolysis bio-chars. Chem. Eng. J. 236, 513–528.

Mohan, D., Sarswat, A., Ok, Y.S., Pittman, C.U., 2014b. Organic and inorganic contaminants removal from water with biochar, a renewable, low cost and sustainable adsorbent – a critical review. Bioresour. Technol. 160, 191–202.

Mukherjee, A., Zimmerman, A.R., Harris, W., 2011. Surface chemistry variations among a series of laboratory-produced biochars. Geoderma 163, 247–255.

Murray, H.H., 1991. Overview — clay mineral applications. Appl. Clay Sci. 5, 379–395.

Novak, J.M.L. Isabel, Xing, Baoshan, Gaskin, Julia W., Steiner, Christoph, Das, K.C., Ahmedna, Mohamed, Rehrah, Djaafar, Watts, Donald W., Busscher, Warren J., Schomberg, Harry, 2009. Characterization of designer biochar produced at different temperatures and their effects on a loamy sand. Ann. Environ. Sci. 3, 195–206.

Oh, G.H., Park, C.R., 2002. Preparation and characteristics of rice-straw-based porous carbons with high adsorption capacity. Fuel 81, 327–336.

Ok, Y.S., Chang, S.X., Gao, B., Chung, H.-J., 2015. SMART biochar technology – a shifting paradigm towards advanced materials and healthcare research. Environ. Technol. Innovation 4, 206–209.

Paria, S., 2008. Surfactant-enhanced remediation of organic contaminated soil and water. Adv. Colloid Interface Sci. 138, 24–58.

Park, J.-H., Ok, Y.S., Kim, S.-H., Cho, J.-S., Heo, J.-S., Delaune, R.D., Seo, D.-C., 2015a. Competitive adsorption of heavy metals onto sesame straw biochar in aqueous solutions. Chemosphere 142, 77–83.

Park, J.H., Ok, Y.S., Kim, S.H., Cho, J.S., Heo, J.S., Delaune, R.D., Seo, D.C., 2015b. Evaluation of phosphorus adsorption capacity of sesame straw biochar on aqueous solution: influence of activation methods and pyrolysis temperatures. Environ. Geochem Health 1–15.

Qian, K., Kumar, A., Zhang, H., Bellmer, D., Huhnke, R., 2015. Recent advances in utilization of biochar. Renew. Sustain. Energy Rev. 42, 1055–1064.

Qian, W., Zhao, A.-z., Xu, R.-k., 2013. Sorption of As(V) by aluminum-modified crop straw-derived biochars. Water Air Soil Pollut. 224, 1–8.

Rajapaksha, A.U., Vithanage, M., Ahmad, M., Seo, D.-C., Cho, J.-S., Lee, S.-E., Lee, S.S., Ok, Y.S., 2015. Enhanced sulfamethazine removal by steam-activated invasive plant-derived biochar. J. Hazard. Mater. 290, 43–50.

Rajapaksha, A.U., Vithanage, M., Lim, J.E., Ahmed, M.B.M., Zhang, M., Lee, S.S., Ok, Y.S., 2014a. Invasive plant-derived biochar inhibits sulfamethazine uptake by lettuce in soil. Chemosphere 111, 500–504.

Rajapaksha, A.U., Vithanage, M., Weerasooriya, R., Dissanayake, C.B., 2012. Surface complexation of nickel on iron and aluminum oxides: a comparative study with single and dual site clays. Colloids Surf. A Physicochem. Eng. Aspects 405, 79–87.

Rajapaksha, A.U., Vithanage, M., Zhang, M., Ahmad, M., Mohan, D., Chang, S.X., Ok, Y.S., 2014b. Pyrolysis condition affected sulfamethazine sorption by tea waste biochars. Bioresour. Technol. 166, 303–308.

Regmi, P., Garcia Moscoso, J.L., Kumar, S., Cao, X., Mao, J., Schafran, G., 2012. Removal of copper and cadmium from aqueous solution using switchgrass biochar produced via hydrothermal carbonization process. J. Environ. Manag. 109, 61–69.

Ren, J., Li, N., Li, L., An, J.-K., Zhao, L., Ren, N.-Q., 2015. Granulation and ferric oxides loading enable biochar derived from cotton stalk to remove phosphate from water. Bioresour. Technol. 178, 119–125.

Saleh, M.M., 2006. On the removal of cationic surfactants from dilute streams by granular charcoal. Water Res. 40, 1052–1060.

Samsuri, A.W., Sadegh-Zadeh, F., Seh-Bardan, B.J., 2013. Adsorption of As(III) and As(V) by Fe coated biochars and biochars produced from empty fruit bunch and rice husk. J. Environ. Chem. Eng. 1, 981–988.

Santhanalakshmi, J., Balaji, S., 1996. Adsorption studies of nonionic surfactants on charcoal and alumina in aromatic solvents. J. Colloid Interface Sci. 179, 517–521.

Shafeeyan, M.S., Daud, W.M.A.W., Houshmand, A., Shamiri, A., 2010. A review on surface modification of activated carbon for carbon dioxide adsorption. J. Anal. Appl. Pyrolysis 89, 143–151.

Singh, B.P., Hatton, B.J., Singh, B., Cowie, A.L., Kathuria, A., 2010. Influence of biochars on nitrous oxide emission and nitrogen leaching from two contrasting soils. J. Environ. Qual. 39, 1224–1235.

Song, Z., Lian, F., Yu, Z., Zhu, L., Xing, B., Qiu, W., 2014. Synthesis and characterization of a novel MnOx-loaded biochar and its adsorption properties for Cu^{2+} in aqueous solution. Chem. Eng. J. 242, 36–42.

Stavropoulos, G.G., Samaras, P., Sakellaropoulos, G.P., 2008. Effect of activated carbons modification on porosity, surface structure and phenol adsorption. J. Hazard. Mater. 151, 414–421.

Sun, K., Jian-chun, J., Dan-dan, C., 2011. Preparation of activated carbon with highly developed mesoporous structure from Camellia oleifera shell through water vapor gasification and phosphoric acid modification. Biomass Bioenergy 35, 3643–3647.

Tan, Z., Qiu, J., Zeng, H., Liu, H., Xiang, J., 2011. Removal of elemental mercury by bamboo charcoal impregnated with H_2O_2. Fuel 90, 1471–1475.

Tripathy, S.S., Kanungo, S.B., 2005. Adsorption of Co^{2+}, Ni^{2+}, Cu^{2+} and Zn^{2+} from 0.5 M NaCl and major ion sea water on a mixture of δ-MnO$_2$ and amorphous FeOOH. J. Colloid Interface Sci. 284, 30–38.

Uchimiya, M., Chang, S., Klasson, K.T., 2011. Screening biochars for heavy metal retention in soil: role of oxygen functional groups. J. Hazard. Mater. 190, 432–441.

Usman, A., Sallam, A., Al-Omran, A., El-Naggar, A., Alenazi, K., Nadeem, M., Al-Wabel, M., 2013. Chemically modified biochar produced from conocarpus wastes: an efficient sorbent for Fe(II) removal from acidic aqueous solutions. Adsorpt. Sci. Technol. 31, 625–640.

Van Vinh, N., Zafar, M., Behera, S.K., Park, H.S., 2015. Arsenic(III) removal from aqueous solution by raw and zinc-loaded pine cone biochar: equilibrium, kinetics, and thermodynamics studies. Int. J. Environ. Sci. Technol. 12, 1283–1294.

Vithanage, M., Chandrajith, R., Bandara, A., Weerasooriya, R., 2006. Mechanistic modeling of arsenic retention on natural red earth in simulated environmental systems. J. Colloid Interface Sci. 294, 265–272.

Vithanage, M., Rajapaksha, A.U., Ahmad, M., Uchimiya, M., Dou, X., Alessi, D.S., Ok, Y.S., 2015a. Mechanisms of antimony adsorption onto soybean stover-derived biochar in aqueous solutions. J. Environ. Manag. 151, 443–449.

Vithanage, M., Rajapaksha, A.U., Tang, X., Thiele-Bruhn, S., Kim, K.H., Lee, S.E., Ok, Y.S., 2014. Sorption and transport of sulfamethazine in agricultural soils amended with invasive-plant-derived biochar. J. Environ. Manag. 141, 95–103.

Vithanage, M., Rajapaksha, A.U., Zhang, M., Thiele-Bruhn, S., Lee, S.S., Ok, Y.S., 2015b. Acid-activated biochar increased sulfamethazine retention in soils. Environ. Sci. Pollut. Res. 22, 2175–2186.

Wang, M.C., Sheng, G.D., Qiu, Y.P., 2014. A novel manganese-oxide/biochar composite for efficient removal of lead(II) from aqueous solutions. Int. J. Environ. Sci. Technol. 1–8.

Wang, S., Gao, B., Li, Y., Mosa, A., Zimmerman, A.R., Ma, L.Q., Harris, W.G., Migliaccio, K.W., 2015a. Manganese oxide-modified biochars: preparation, characterization, and sorption of arsenate and lead. Bioresour. Technol. 181, 13–17.

Wang, S., Gao, B., Zimmerman, A.R., Li, Y., Ma, L., Harris, W.G., Migliaccio, K.W., 2015b. Removal of arsenic by magnetic biochar prepared from pinewood and natural hematite. Bioresour. Technol. 175, 391–395.

Wang, Y., Wang, X.J., Liu, M., Wang, X., Wu, Z., Yang, L.Z., Xia, S.Q., Zhao, J.F., 2012. Cr(VI) removal from water using cobalt-coated bamboo charcoal prepared with microwave heating. Ind. Crops Prod. 39, 81–88.

Woolf, D., Amonette, J.E., Street-Perrott, F.A., Lehmann, J., Joseph, S., 2010. Sustainable biochar to mitigate global climate change. Nat. Commun. 1.

Xiong, Z., Shihong, Z., Haiping, Y., Tao, S., Yingquan, C., Hanping, C., 2013. Influence of NH$_3$/CO$_2$ modification on the characteristic of biochar and the CO$_2$ capture. Bioenerg. Res. 6, 1147–1153.

Xue, Y., Gao, B., Yao, Y., Inyang, M., Zhang, M., Zimmerman, A.R., Ro, K.S., 2012. Hydrogen peroxide modification enhances the ability of biochar (hydrochar) produced from hydrothermal carbonization of peanut hull to remove aqueous heavy metals: batch and column tests. Chem. Eng. J. 200–202, 673–680.

Yakout, S.M., Daifullah, A.E.H.M., El-Reefy, S.A., 2015. Pore structure characterization of chemically modified biochar derived from rice straw. Environ. Eng. Manag. J. 14, 473–480.

Yan, J., Han, L., Gao, W., Xue, S., Chen, M., 2015a. Biochar supported nanoscale zerovalent iron composite used as persulfate activator for removing trichloroethylene. Bioresour. Technol. 175, 269–274.

Yan, L.-G., Xu, Y.-Y., Yu, H.-Q., Xin, X.-D., Wei, Q., Du, B., 2010. Adsorption of phosphate from aqueous solution by hydroxy-aluminum, hydroxy-iron and hydroxy-iron–aluminum pillared bentonites. J. Hazard. Mater. 179, 244–250.

Yan, L., Kong, L., Qu, Z., Li, L., Shen, G., 2015b. Magnetic biochar decorated with ZnS nanocrytals for Pb (II) removal. ACS Sustain. Chem. Eng. 3, 125–132.

Yang, G.-X., Jiang, H., 2014. Amino modification of biochar for enhanced adsorption of copper ions from synthetic wastewater. Water Res. 48, 396–405.

Yang, R., Liu, G., Xu, X., Li, M., Zhang, J., Hao, X., 2011. Surface texture, chemistry and adsorption properties of acid blue 9 of hemp (Cannabis sativa L.) bast-based activated carbon fibers prepared by phosphoric acid activation. Biomass Bioenergy 35, 437–445.

Yao, Y., Gao, B., Chen, J., Yang, L., 2013a. Engineered biochar reclaiming phosphate from aqueous solutions: mechanisms and potential application as a slow-release fertilizer. Environ. Sci. Technol. 47, 8700–8708.

Yao, Y., Gao, B., Chen, J., Zhang, M., Inyang, M., Li, Y., Alva, A., Yang, L., 2013b. Engineered carbon (biochar) prepared by direct pyrolysis of Mg-accumulated tomato tissues: characterization and phosphate removal potential. Bioresour. Technol. 138, 8–13.

Yao, Y., Gao, B., Fang, J., Zhang, M., Chen, H., Zhou, Y., Creamer, A.E., Sun, Y., Yang, L., 2014. Characterization and environmental applications of clay–biochar composites. Chem. Eng. J. 242, 136–143.

Yao, Y., Gao, B., Inyang, M., Zimmerman, A.R., Cao, X., Pullammanappallil, P., Yang, L., 2011a. Biochar derived from anaerobically digested sugar beet tailings: characterization and phosphate removal potential. Bioresour. Technol. 102, 6273–6278.

Yao, Y., Gao, B., Inyang, M., Zimmerman, A.R., Cao, X., Pullammanappallil, P., Yang, L., 2011b. Removal of phosphate from aqueous solution by biochar derived from anaerobically digested sugar beet tailings. J. Hazard. Mater. 190, 501–507.

Yong, S., Bolan, N.S., Lombi, E., Skinner, W., 2013. Synthesis and characterization of thiolated chitosan beads for removal of Cu(II) and Cd(II) from wastewater. Water Air Soil Pollut. 224, 1–12.

Yong, S.K., Bolan, N.S., Lombi, E., Skinner, W., 2012. Sulfur-containing chitin and chitosan derivatives as trace metal adsorbents: a review. Crit. Rev. Environ. Sci. Technol. 43, 1741–1794.

Zhang, J., Huang, Z.-H., Lv, R., Yang, Q.-H., Kang, F., 2009. Effect of growing CNTs onto bamboo charcoals on adsorption of copper ions in aqueous solution. Langmuir 25, 269–274.

Zhang, M., Gao, B., 2013. Removal of arsenic, methylene blue, and phosphate by biochar/AlOOH nanocomposite. Chem. Eng. J. 226, 286–292.

Zhang, M., Gao, B., Varnoosfaderani, S., Hebard, A., Yao, Y., Inyang, M., 2013a. Preparation and characterization of a novel magnetic biochar for arsenic removal. Bioresour. Technol. 130, 457–462.

Zhang, M., Gao, B., Yao, Y., Xue, Y., Inyang, M., 2012a. Synthesis of porous MgO-biochar nanocomposites for removal of phosphate and nitrate from aqueous solutions. Chem. Eng. J. 210, 26–32.

Zhang, M., Gao, B., Yao, Y., Xue, Y., Inyang, M., 2012b. Synthesis, characterization, and environmental implications of graphene-coated biochar. Sci. Total Environ. 435–436, 567–572.

Zhang, X., Zhang, S., Yang, H., Feng, Y., Chen, Y., Wang, X., Chen, H., 2014a. Nitrogen enriched biochar modified by high temperature CO_2-ammonia treatment: characterization and adsorption of CO_2. Chem. Eng. J. 257, 20–27.

Zhang, X.N., Mao, G.Y., Jiao, Y.B., Shang, Y., Han, R.P., 2014b. Adsorption of anionic dye on magnesium hydroxide-coated pyrolytic bio-char and reuse by microwave irradiation. Int. J. Environ. Sci. Technol. 11, 1439–1448.

Zhang, Z., Wang, X., Wang, Y., Xia, S., Chen, L., Zhang, Y., Zhao, J., 2013b. Pb(II) removal from water using Fe-coated bamboo charcoal with the assistance of microwaves. J. Environ. Sci. 25, 1044–1053.

Zhao, R.-S., Liu, Y.-L., Chen, X.-F., Yuan, J.-P., Bai, A.-Y., Zhou, J.-B., 2013. Preconcentration and determination of polybrominated diphenyl ethers in environmental water samples by solid-phase microextraction with Fe_3O_4-coated bamboo charcoal fibers prior to gas chromatography–mass spectrometry. Anal. Chim. Acta 769, 65–71.

Zhou, Y., Gao, B., Zimmerman, A.R., Fang, J., Sun, Y., Cao, X., 2013. Sorption of heavy metals on chitosan-modified biochars and its biological effects. Chem. Eng. J. 231, 512–518.